Yang *et al. Soft Sci.* **2025**, *5*, 33
DOI: 10.20517/ss.2025.12

Soft Science

Mini Review

Open Access

Check for updates

MXene-based flexible sensors for wearable applications

Wenjie Yang[1,2], Fenglu Liu[1], Yongxiang Lin[3], Jun Wang[2,*], Cheng Zhang[2,*], Huanyu Cheng[4,*], Huamin Chen[2,5,*]

[1]College of Mechanical and Electrical Engineering, Fujian Agriculture and Forestry University, Fuzhou 350108, Fujian, China.
[2]College of Materials and Chemical Engineering, Fuzhou Institute of Oceanography, Minjiang University, Fuzhou 350108, Fujian, China.
[3]GRG Metrology & Test (Fuzhou) Co., Ltd., Fuzhou 350108, Fujian, China.
[4]Department of Engineering Science and Mechanics, The Pennsylvania State University, University Park, PA 16802, USA.
[5]Institute of Semiconductors, Chinese Academy of Sciences, Beijing 100083, China.

[*]**Correspondence to:** Prof. Jun Wang, Prof. Cheng Zhang, College of Materials and Chemical Engineering, Fuzhou Institute of Oceanography, Minjiang University, No. 200, Xiyuangong Road, Shangjie Town, Minhou County, Fuzhou 350108, Fujian, China. E-mail: wangjun2@mju.edu.cn; zhangcheng@mju.edu.cn; Prof. Huanyu Cheng, Department of Engineering Science and Mechanics, The Pennsylvania State University, 201 Old Main, University Park, PA 16802, USA. E-mail: huanyu.cheng@psu.edu; Assoc. Prof. Huamin Chen, Institute of Semiconductors, Chinese Academy of Sciences, No. A35, Qinghua East Road, Haidian District, Beijing 100083, China. E-mail: chenhuamin@semi.ac.cn

How to cite this article: Yang, W.; Liu, F.; Lin, Y.; Wang, J.; Zhang, C.; Cheng, H.; Chen, H. MXene-based flexible sensors for wearable applications. *Soft Sci.* **2025**, *5*, 33. https://dx.doi.org/10.20517/ss.2025.12

Received: 8 Apr 2025 **First Decision:** 10 Jun 2025 **Revised:** 7 Jul 2025 **Accepted:** 8 Jul 2025 **Published:** 15 Jul 2025

Academic Editor: YongAn Huang **Copy Editor:** Ting-Ting Hu **Production Editor:** Ting-Ting Hu

Abstract

In recent years, with the rapid advances in flexible electronic device technology and the demand for a wide range of applications, MXene has emerged as an ideal multifunctional 2D nanomaterial for next-generation flexible sensors. It is unique in that it combines metallic conductivity, tunable surface chemistry and mechanical flexibility. These properties allow MXene to exhibit superior performance compared to other 2D materials, including graphene, in the fabrication of flexible sensors. This review summarizes the recent research progress in the field of different modes of flexible MXene-based sensors, including single-mode sensors, dual-mode sensors, and multimode sensors. First, MXene-based flexible sensors for pressure, strain, temperature, humidity, gas, and photoelectricity are described in detail. Then, the research progress of MXene in the field of flexible dual-mode sensors is systematically described, the key performance parameters of multimode sensors are summarized, and the applications of MXene-based flexible sensors in various fields are described. Finally, the future trends of flexible MXene-based sensors and the challenges they face are discussed, aiming to provide useful insights for future wearable applications.

Keywords: MXene, flexible sensor, multimode, wearable electronics, health monitoring

INTRODUCTION

The innovation of nanocomposite materials and advanced manufacturing techniques has spurred the rapid development of high-performance flexible sensors and wearable devices in robot perception[1], electronic skin[2,3], artificial intelligence[4], human-computer interaction[5,6], and human health monitoring[7,8]. The single-modal sensors detect only one input signal (e.g., pressure sensors[9,10] and temperature sensors[11], humidity sensors[12], and gas sensors[13]) and have some limitations. In order to overcome the limitations of single-mode sensors with a single function, multimode sensors have received a lot of attention from researchers. Flexible multimode sensors can detect two or more input signals. Multimodal sensing can be achieved by combining flexible sensing materials with different modes vertically or zonally in the same sensor, which can collect different signals separately. However, this method has significant challenges, such as complex equipment structures, cumbersome and expensive manufacturing procedures, and large volumes, which considerably limit its practical application.

Conductive nanomaterials, including carbonaceous fillers[14-17], intrinsic conductive polymers[18,19], and nano metals[20,21], are extensively used for designing and fabricating flexible sensors. Among the many alternatives, two-dimensional (2D) materials stand out for their extraordinary potential due to their extraordinarily large specific surface area, excellent mechanical properties, tunable structural properties, and outstanding flexibility. Compared with traditional bulk materials, 2D materials are more suitable for human-like sensing applications due to their larger surface area[22], higher carrier mobility[23,24], and good flexibility[25,26]. MXene is a new class of 2D layered nanomaterials, which belongs to the derivatives of $M_{n+1}AX_n$ phase material (MAX phase for short). MAX phase is a class of ternary layered compounds, where M is an early transition metal (e.g., Ti, V, Nb, Mo), A is an element of the main group of III and IV (e.g., Al, Si), and X is either C or N, with n = 1,2,3. In the MAX direction, the ionic and covalent bonding interactions between M and X are stronger than the M-A metallic bonding, so MXene can be obtained by selectively destroying the "A" layer atoms by strong etching. The chemical formula of MXene obtained by precursor MAX etching is $M_{n+1}X_nT_x$, (n = 1,2,3) representing the three structures [Figure 1A][27,28], where M stands for early transition metals (e.g., Ti, Zr, V, Mo, etc., elements in blue in Figure 1A); X represents C or N elements (elements in gray in Figure 1A); T_x denotes surface functional groups (e.g., -OH, -F, -O, -Cl elements in orange in Figure 1A). MXenes [Figure 1A], their MAX phase precursors, and metal ions embedded in MXene [Figure 1B] together illustrate the basic principles of chemistry, demonstrating how diverse nanomaterials can be constructed by using these elements as basic building blocks. Currently, the synthesis techniques of MXene mainly include hydrofluoric acid (HF) etching, *in situ* HF generation etching, electrochemical etching, alkaline etching, and molten salt etching [Figure 1C]. It has good hydrophilicity, excellent electrical conductivity, extraordinary mechanical properties, abundant surface functional groups, and high specific surface area, it is commonly used in photothermal conversion[29], nanogenerators[30], sensors[31-33], electromagnetic interference (EMI) shielding[34,35] and energy storage[36,37]. MXene surface can be chemically modified to tailor their properties for specific sensing applications. MXene has received considerable research attention as an ideal candidate for flexible sensors.

This review summarizes the latest research progress of flexible sensors based on MXene-based materials for wearable applications [Figure 2]. First, the fundamental principles of various MXene-based single-mode flexible sensors are systematically and comprehensively illustrated, emphasizing their definition and principle. Then, the latest progress in MXene-based dual-mode and multimodal flexible sensors is further reviewed, summarizing material optimization, performance enhancement, and practical applications. Finally, some challenges and opportunities for MXene-based flexible sensors are summarized. The paper concludes with directions and important insights for the future development of MXene-based flexible sensors.

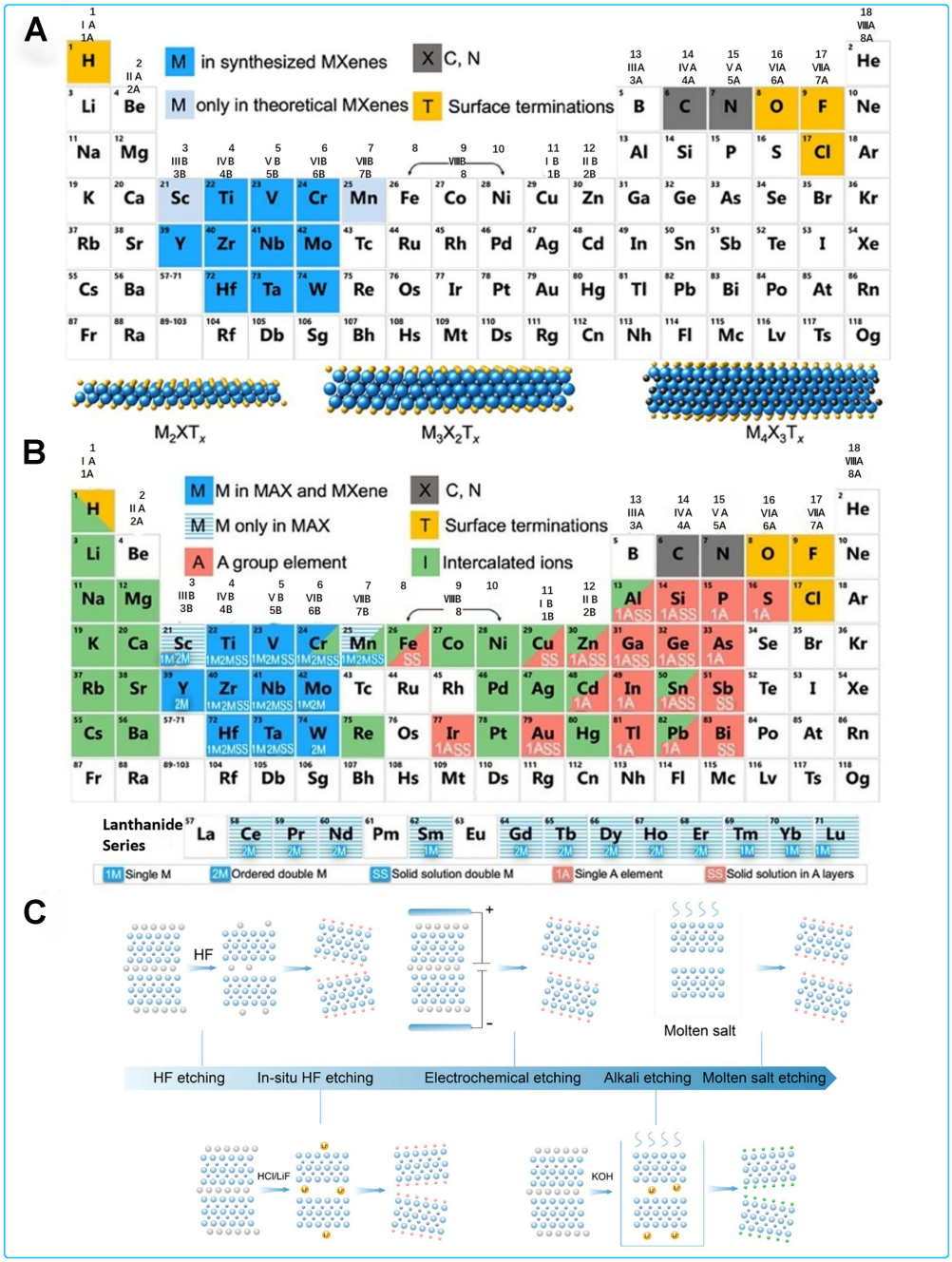

Figure 1. Synthesis of MXene. (A) The constituent elements of MXene, with the three structures of MXene at the bottom; (B) Elements employed in synthesizing MAX phases, MXenes, and their intercalated ions. The blue-striped element is limited to the MAX phase system, whose MXene has still not been successfully prepared. The red background element points to the etchability of A element in the MAX phase. The green background corresponds to the set of cations for which MXene embedding has been accomplished. Reproduced with permission[27]. Copyright 2019, American Chemical Society; (C) Preparation method of MXene. Reproduced with permission[28]. Copyright 2023, Wiley. MAX: $M_{n+1}AX_n$ phase material.

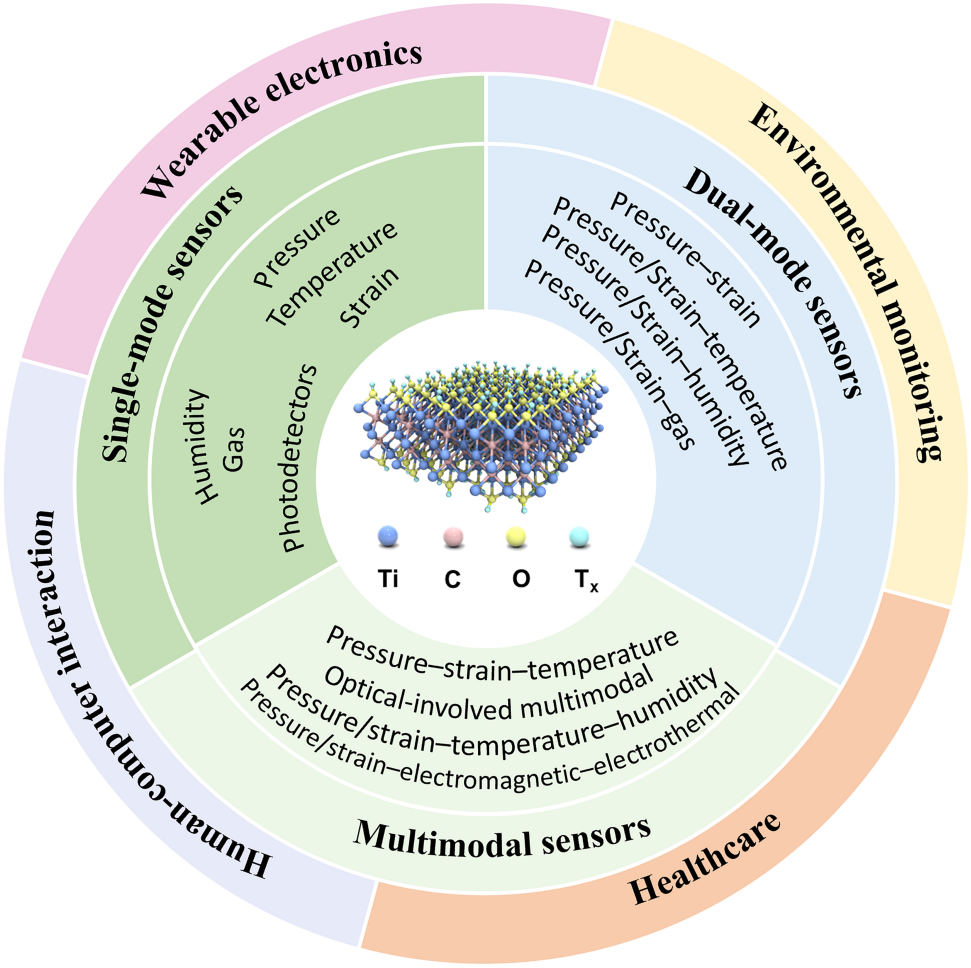

Figure 2. MXene-based materials for different modal sensors and application fields.

SINGLE-MODAL SENSORS

As the fundamental building blocks for flexible sensing systems, single-mode sensors are desirable to accurately measure applied physical quantities such as pressure, strain, temperature, humidity, gas concentration, and optical signals for precise perception of complex environments. Therefore, the latest research progress on MXene-based flexible single-mode sensors is first summarized herein.

Pressure sensors

Aerogels and sponges are popular in flexible pressure sensors due to lightweight, high porosity and elasticity, and large surface area. The deformation of porous structures under external stress alters the distance between conductive skeletons and often increases the conductive pathway. For instance, with the help of Amino carbon nanotubes (NH_2-CNTs) to allow uniform adhesion and distribution of MXenes onto the melamine sponge skeleton to promote the transfer of electrons and protons, the pressure sensor demonstrates high sensitivity, rapid response/recovery, extremely low detection limit, and exceptional stability/reproducibility[38]. Further coating of the superhydrophobic SiO_2 nanoparticles provides the sensor with waterproof properties. Reduced graphene oxide (rGO) with a high specific surface area is combined with MXene of excellent conductivity to prepare a piezoresistive sensor with a hierarchical porous structure [Figure 3A][39]. The large rGO sheets wrapped around the MXene prevent its oxidation, whereas the MXene

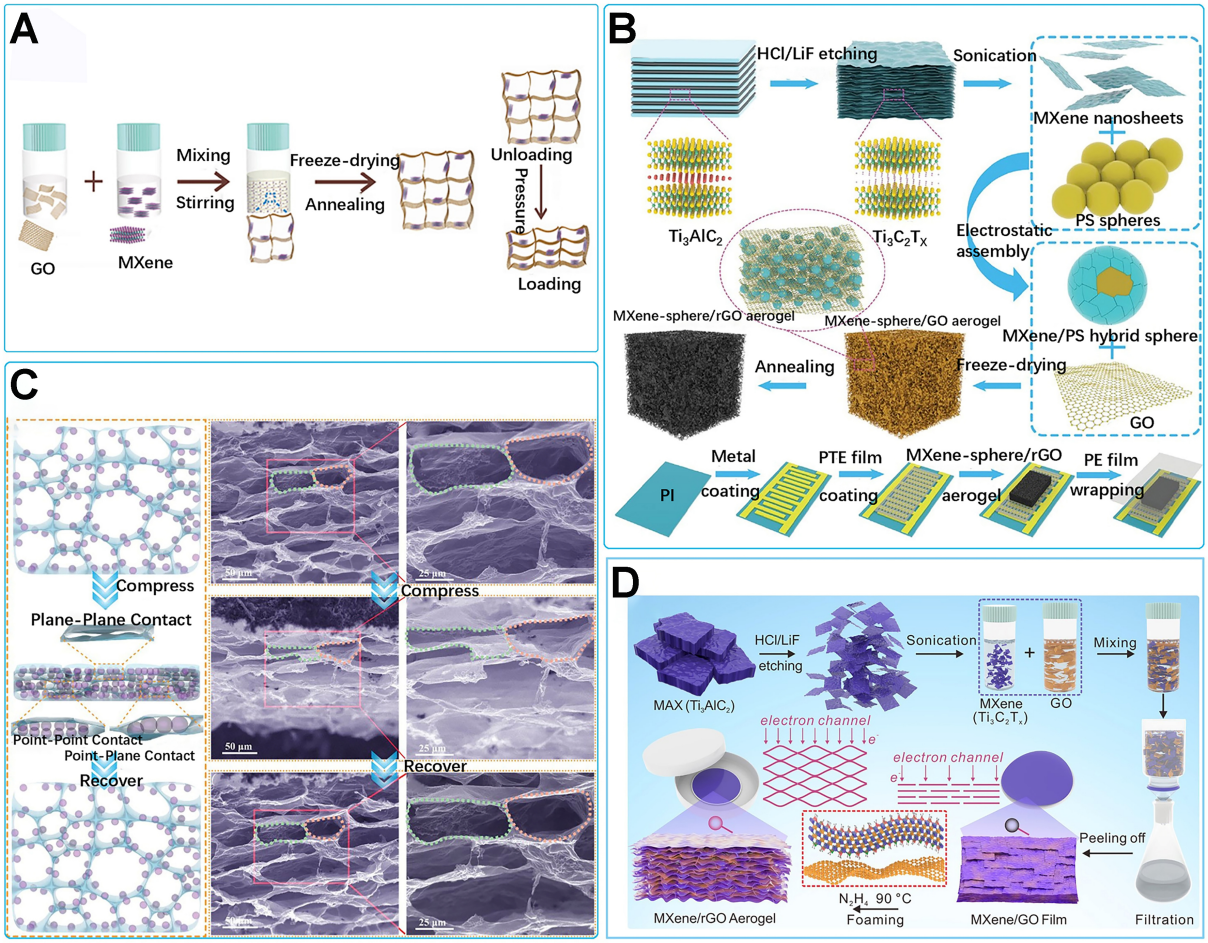

Figure 3. Pressure sensors and sensing mechanisms. (A) Schematic of sensor preparation. Reproduced with permission[39]. Copyright 2018, American Chemical Society; (B) Preparation of composite aerogels and their sensors; (C) Schematic of the sensing mechanism and internal microstructure of pressure sensor. Reproduced with permission[32]. Copyright 2019, Wiley; (D) Preparation of sensors. Reproduced with permission[41]. Copyright 2023, American Chemical Society. GO: Graphene oxide; rGO: reduced graphene oxide; PS: polystyrene; PE: polyethylene; PTE: polyethylene terephthalate; PI: polyimide.

contributes to the improved reversibility and compressive strength of the aerogel due to its high Young's modulus. The aerogel can be compressed to more than 60%, and recover to its original shape after release. This MXene/rGO aerogel exhibits a sensitivity of 22.56 kPa^{-1} and excellent stability over 10,000 cycles.

The design of microstructure is key to enhancing the performance of pressure sensors (e.g., sensitivity particularly under low pressure conditions). Hollow MXene spheres were prepared by the template method and then combined with graphene oxide (GO) to prepare MXene/rGO composite aerogels [Figure 3B][32]. The hollow MXene spheres come into contact with each other in a point-to-point manner or with the surface of the rGO flakes in a point-to-plane manner under low pressures, whereas microstructures form face-to-face contact to result in higher sensitivity under high pressures [Figure 3C]. Due to the additional contact mode that occurs within the aerogel during compression, pressure sensors based on this composite aerogel have a sensitivity of up to 609 kPa^{-1}. Similarly, the piezoresistive pressure sensor prepared with a three-dimensional porous structure using foam as the framework[40] improves the sensitivity and response speed of the sensor, due to the fact that more conductive pathways form internally under pressure. MXene layer spacing is prone to self-stacking, resulting in narrow electronic channels and weak conductance

changes under external pressure, making it difficult to realize high-sensitivity sensing. In order to solve this problem, Cheng *et al.* prepared MXene/rGO aerogel by rapid gas foaming technology, which formed a pore structure with adjustable interlayer spacing to expand the electron transport channel [Figure 3D][41]. The enriched interlayer network provided more electron transport channels when subjected to pressure, which enabled the sensor to exhibit a high sensitivity of 1,799.5 kPa^{-1}.

Strain sensors

The piezoresistive effect also allows the sensor to detect tensile or compressive strains that change the conductive path and resistance values. Crack and fracture may also occur upon tensile strain[42,43] to hinder the flow of electrons for increased resistance, before complete damage of the sensor to cause a sharp increase in resistance. The sensitivity of a strain sensor is defined as gauge factor (GF) = $((R-R_0)/R_0)/\varepsilon$, where ε is the strain, R_0 is the resistance without strain, and R is the resistance under strain. Inspired by the overlapping tiles on the roofs of ancient palaces, a flexible/wearable strain sensor with tile-like, hierarchically stacked, layered MXene/polyaniline fiber (PANIF) sheets exhibits excellent sensitivity with a GF of up to 2,369.1, a broad sensing range of 80%, a low detection limit of 0.1538%, and outstanding cycling stability [Figure 4A][44]. First, the MXene aqueous suspension is spread on the substrate to form a thin MXene film. Then, the PANIF aqueous suspension is spread on the MXene film-coated substrate. The film is stretched to 60% strain to create microcracks and then coated by MXene and PANIF aqueous suspensions. Finally, the film is stretched to 100% strain to create more microcracks and gradually released to its original state, forming a tile-like, hierarchically stacked strain sensor. The increased sensing range is provided by PANIF and overlapping microstructures to ensure the connectivity of the conductive paths upon stretching. The break of the PANIFs, along with widened spacing and increased density of the microcracks on the sensing layer, results in enhanced sensitivity at higher strains. A woven structure formed by interconnecting MXene nanolayers with CNTs allows the sandwiched strain sensor to detect small deformations of 0.1%, along with excellent reliability and stability over 5,000 cycles [Figure 4B][45]. The sensor has a GF of up to 772.6 and a thin sensing layer size (< 2um). The sensing range (30%-130%) can be adjusted by adjusting the concentration of the sensing material and controlling the number of sprays. The flexible strain sensor with conductive MXene/polypyrrole (PPy)/hydroxyethyl cellulose (HEC) sandwiched between polydimethylsiloxane (PDMS) substrate and encapsulation can also exhibit increased sensitivity over a broad linear strain detection range, high reproducibility, and swift response and recovery[9]. With conductive PPy added to increase the sensing range, the sensor exhibits a sensitivity or GF of 357.5 over a large detection range from 12% to 94%, repeatability of over 1,300 cycles, and a reasonably fast response/recovery time of 300 ms.

Temperature sensors

MXene has not only metal-like high electrical conductivity and unique layered nanostructure, but also excellent thermal conductivity, large specific surface area and abundant surface groups, making it an ideal material for temperature sensing[46-49]. Due to the electronic properties of MXene itself, an increase in temperature leads to an increase in carrier concentration and an increase in electron mobility, resulting in a decrease in resistance. In addition, when MXene is combined with a flexible substrate with a large coefficient of expansion, thermal expansion of the substrate will lead to changes in the conductive network, which will lead to changes in resistance.

The flexible temperature sensor based on MXene shows excellent sensitivity of 986 $°C^{-1}$ and can detect distance from the fingertip due to the variations in the thermal field[50]. It can also distinguish small bottles containing ice water, warm water, and hot water, along with the infrared laser irradiation of different powers [Figure 4C]. Combining MXene with sodium alginate hydrogel successfully prepares flexible temperature sensors with a high sensitivity of 3,244% $°C^{-1}$ over a wide temperature range from -20 to 100 °C

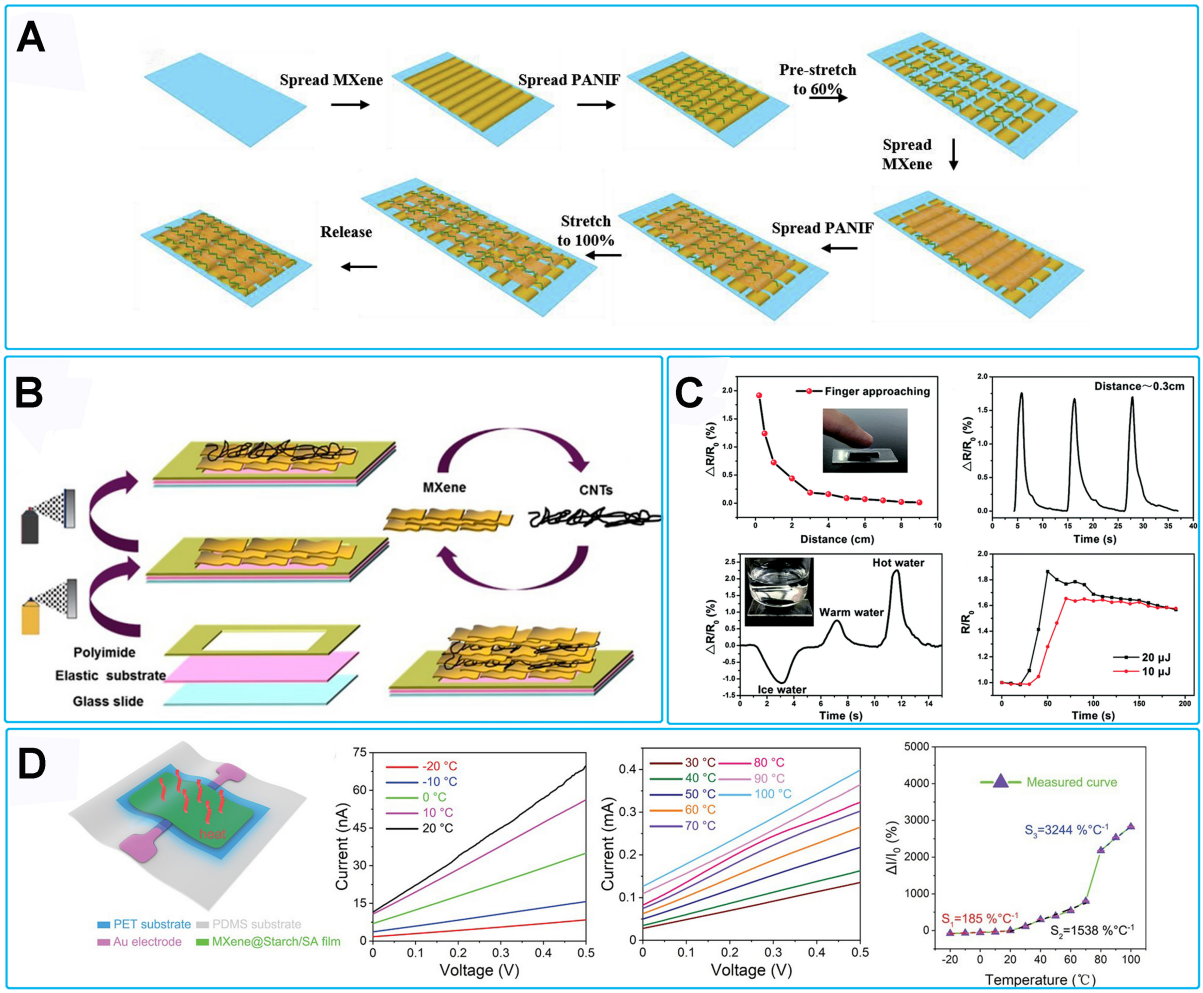

Figure 4. Strain sensor and temperature sensing performance. (A and B) Strain sensor; (C and D) Temperature sensing performance. (A) Nanocomposite synthesis. Reproduced with permission[44].Copyright 2020, Elsevier; (B) Manufacturing of sensing layer. Reproduced with permission[45].Copyright 2017, American Chemical Society; (C) Excellent performance of temperature sensors in sensitivity, repeatability, temperature measurement range, and infrared response capability. Reproduced with permission[50].Copyright 2019, Royal Society of Chemistry; (D) Schematic of the sensor, along with its I-V curve and sensitivity of within the sensing range. Reproduced with permission[51].Copyright 2012, Wiley. PANIF: Polyaniline fiber; CNTs: carbon nanotubes; PDMS: polydimethylsiloxane; SA: sodium alginate; PET: polyethylene terephthalate.

[Figure 4D][51]. The flexible thermosensitive sensor based on a hybrid material composed of CNTs and MXene also exhibits excellent temperature resolution of 0.3 °C, a wide detection range from -20 to 220 °C, and stability over 2,000 bending cycles[52]. Enhanced sensitivity is also observed when compared to the temperature sensor based on epoxy/multiwalled carbon nanotubes (MWCNTs) (0.52% $°C^{-1}$ *vs.* 0.036% $°C^{-1}$).

Humidity sensors

Humidity reflects physical activities and subtle changes in physiological functions, so highly sensitive and stable sensing of humidity is of considerable significance. The abundance of hydrophilic active sites on the surface of MXene makes it ideally suited for moisture sensing[53,54]. The absorption (or desorption) of water molecules onto (or from) MXene nanosheets changes the interlayer spacing of MXene to cause conductivity variations[22,55].

The flexible humidity sensor with a nacre-inspired "brick and mortar" structure composed of MXene and 1D 2,2,6,6-tetramethyl-1-piperidinyloxy (TEMPO)-oxidized cellulose nanofibers (TOCNF) shows a maximum response of 90% and long-term stability at 97% relative humidity (RH) over 10 days[56]. Rich hydrophilic groups on the surfaces of MXenes allow them to stably disperse in aqueous environments, positively impacting the wettability and breathability of fabrics when modified with MXenes. The large interlayer spacing of MXenes can effectively load more other functional materials to provide the fabric with multifunctionality. For instance, the MXenes/MWCNT fabric-based humidity sensor exhibits a large response of 265% to 90% RH and remarkable stability under deformation[31]. The response change of 7% from the MXenes/MWCNT-based fabric sensor upon 10% stretching under 80% RH is much smaller than that of 35% from the MXenes-based fabric sensor. Integrating the humidity sensor in a mask identifies human respiration and breathing patterns.

To overcome the low sensitivity and slow response of traditional humidity sensors, MXene was alkalized to form a three-dimensional porous structure, and its surface was subsequently modified with poly(diallyldimethylammonium chloride) (PDDA) to form a composite material (KPMX)[57]. KPMX ink printed on the forked electrode on paper as the moisture sensitive layer is combined with the pre-strain strategy to yield a stretchable paper-based humidity sensor with extraordinary humidity sensing performance for respiratory monitoring [Figure 5A]. The humidity sensing relies on the hydrophilic functional groups of composite materials to attract water molecules. Double hydrogen bonds formed under low humidity facilitate proton transfer via hopping mechanisms. Under high humidity, the interaction between a large number of water molecules and the sensing materials shifts the charge transfer mechanism from simple proton hopping to a complex process involving ion diffusion. The KPMX-based humidity sensor exhibits high sensitivity of 48,813% to 97% RH and fast response/recovery times of 8.794/2.656 s.

However, MXene is susceptible to oxidation in air, which can affect sensor stability. Therefore, it is of high interest to exploit the oxygen functional groups and polyethyleneimine/silver nitrate (PEI/$AgNO_3$) cross-linking modification layer sufficiently covers MXene to effectively inhibit the oxidation reaction. By incorporating PEI/$AgNO_3$ into the MXene to refine the interlayer distance and provide abundant hydrophilic functional groups, the resulting paper-based humidity sensor demonstrates enhanced adsorption of water molecules [Figure 5B][58]. The sensor features a response of 819.9% to 97% RH, stable capacitance responses (< 3% changes over 100 cycles), and rapid response/recovery time of 6.9/11.9 s when cycled between 11% and 97% RH and after 30 days of storage, the resistivity increased by only 16.23 μΩ·cm.

Gas sensors

Gas molecules physically or chemically adsorbed on the MXene surface induce electron transfer to cause variations in conductivity and measured resistance[22,59], allowing the detection of gas concentration[60].

The abundant active sites and edge defects on the MXene surface enhance the adsorption capacity of gas molecules[61]. Upon exposure to air, the MXene-based sensor attracts oxygen molecules and extracts electrons from its conduction band, generating oxygen anions. When exposed to reducing ammonia (NH_3), oxygen anions react with NH_3 and release electrons to the conduction band of the sensing material, decreasing the resistance. By dip coating poly(3,4-ethylenedioxythiophene):poly(4-styrenesulfonate) (PEDOT:PSS)/MXene composite on the interdigitated electrode, the gas sensor exhibits a gas response of 36.6% to 100 ppm NH_3 and swift response/recovery of 116/40 s at ambient temperature [Figure 5C][62]. The enhanced performance of the composite-based sensor over pure PEDOT:PSS and MXene-based sensors confirms the synergetic effect between PEDOT:PSS and $Ti_3C_2T_x$ MXene. Similarly, the $Ti_3C_2T_x$/polyaniline-polypropylene (PANI-PP) composite features rapid response/recovery of 115/26 s and enhanced sensitivity

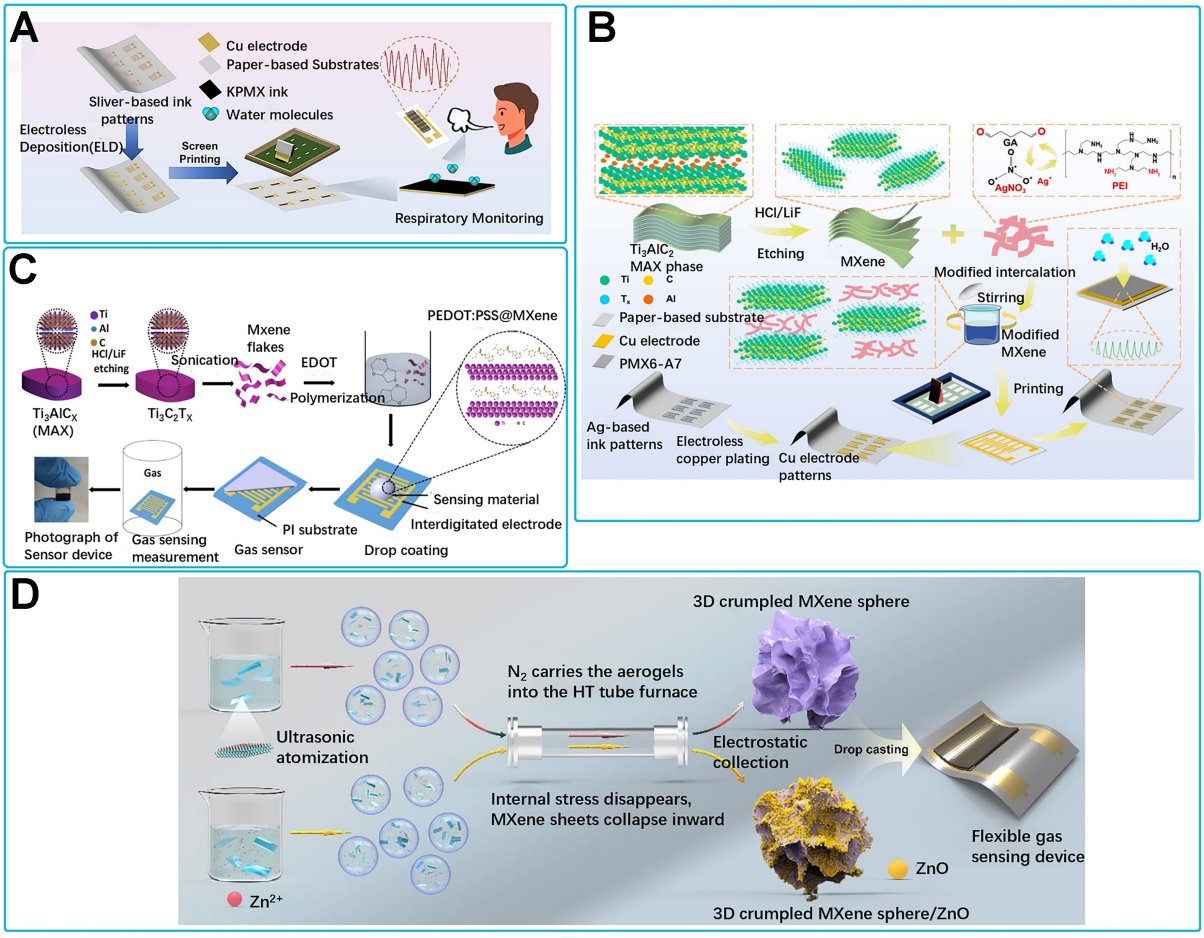

Figure 5. Production humidity sensors and gas sensors. (A and B) Humidity sensor; (C and D) Gas sensor. (A) Humidity sensor fabrication and respiratory monitoring. Reproduced with permission[57]. Copyright 2024, Elsevier; (B) The preparation process of the humidity sensors. Reproduced with permission[58]. Copyright 2022, Elsevier; (C) Fabrication of composite materials and gas sensor. Reproduced with permission[62]. Copyright 2020, American Chemical Society; (D) Fabrication of flexible gas sensor. Reproduced with permission[64]. Copyright 2021, Elsevier. KPMX: "MX" came from "MXene", while "K" indicated that MXene was alkalized by KOH solution, and "P" meant the poly(diallyldimethylammonium chloride) chains loaded on the surface of the $Ti_3C_2T_x$ nanoribbons; PEI: polyethyleneimine; AgNO3: Silver nitrate; PMX6-A7: PEI/MXene/AgNO3, 6 represented the concentrations of PEI and 7 represented the concentrations of AgNO3; PI: polyimide; EDOT: 3,4-ethylenedioxythiophene; PEDOT: poly(3,4-ethylenedioxythiophene); PSS: poly(4-styrenesulfonate); HCl: hydrochloric acid; HT: high-temperature.

of 15.2% to 500 ppm CO_2, which is 6.5 times (or 2.4 times) that of the sensor based on $Ti_3C_2T_x$ (or PANI)[63]. The sensor with a detection range from 25 to 1,500 ppm (response of 22.48% to 1,500 ppm) is further integrated with wireless Bluetooth module into a disposable face mask for respiratory monitoring.

Due to the aggregation of MXene after drying, it loses a large specific surface area, resulting in poor gas sensing performance of gas sensors based on pure 2D MXene nanosheets. ZnO nanoparticles incorporated on 3D crumpled MXene spheres with a high specific surface area provide the resulting room-temperature flexible NO_2 sensor with more active sites [Figure 5D][64]. Compared with sensors based on 3D MXene spheres, sensors based on 3D MXene spheres/ZnO showed an increase in response signal from 27.27% to 41.93% for 100 ppm NO_2, a significant improvement in recovery characteristics from about 30% to about 100%, a reduction in response time from 53 to 34 s, and a reduction in recovery time from over 5 min to 103 s.

Photodetectors

As a key bridge connecting optical and electrical signals, photodetectors are important and irreplaceable in imaging, communication, sensing, and optoelectronics. Owing to their distinctive physicochemical properties and adjustable optical absorption, MXenes comprised of transition metal carbides and nitrides have garnered considerable interest for use in photodetectors.

Combining $Ti_3C_2T_x$ MXene with n-type silicon substrate to form vertical MXene/Si van der Waals heterojunctions [Figure 6A][65]. The MXene-Si heterostructure absorbs photons under light irradiation to excite electron-hole pairs, which separate under the intrinsic electric field within the heterostructure. The holes migrate toward $Ti_3C_2T_x$, while the electrons cross n-Si to reach the metal electrode. This vertical structure promotes efficient separation and transport of photogenerated carriers. The $Ti_3C_2T_x$/n-Si photodetector exhibits excellent photoresponse performance, with a device on/off ratio of 1×10^5, a responsivity of 26.95 mA/W as shown in Figure 6B, and response/recovery times to light of 0.84/1.67 ms [Figure 6C]. Similarly, etched on glass and exposed to oxygen, $Ti_3C_2T_x$ nanosheets are spontaneously partially oxidized to $Ti_3C_2T_x$-TiO_2 thin films, providing the resulting photodetector with a response of 12 uA to ultraviolet light[66]. Many semiconductor 2D layered materials allow the number of layers of the material to be controlled to adjust the bandgap, thus expanding applications in photodetectors. $Ti_3C_2T_x$ MXenes functionalized by $C_{12}H_{26}$ groups exhibit typical layer-dependent bandgap characteristics[67]. Density functional theory (DFT) calculation reveals that the material bandgap gradually decreases as the number of layers increases. Photodetectors composed of different layers of $Ti_3C_2T_x$-$C_{12}H_{26}$ are shown in Figure 6D. The photoresponse properties of the device to a 1,064 nm laser with different power densities are shown in Figure 6E and F.

DUAL-MODAL SENSORS

While the sensitivity to different types of input signals results in MXene-based multimodal sensors, it is often difficult to simultaneously monitor different stimuli with high accuracy due to interference between them. It is highly desirable to exploit sensors that can transduce each stimulus into a separate signal while suppressing the others[68] (e.g., through structural design[69] or new materials[70,71]) and then integrate them together to simultaneously detect multiple stimuli. It is also possible to use machine learning to eliminate signal coupling[15], but a large dataset is often needed with relatively complex algorithms/programming and the underlying mechanism is unclear. Due to the complex coupling, we will focus on the discussion of dual-modal sensors with decoupled sensing.

Pressure-strain sensors

The stretchable pressure-strain sensor based on carbon black/PDMS/MXene yarn electrodes arranged in an orthogonal direction can distinguish the two signals [Figure 7A], by measuring the current response of single (A_1A_2 or B_1B_2) and mutual (A_1B_1 and A_2B_2) electrodes [Figure 7B][72]. Under vertical pressure, the contact area of the sensor expands to increase the current between the mutual electrodes, whereas the current changes in single electrodes are negligible. Meanwhile, the stretching decreases the current in both single and mutual electrodes. When bending along the yarn direction is applied, the corresponding single electrode experiences lateral strain to decrease the current and the other single electrode remains unchanged, with the current from the mutual electrode increased due to increased contact area [Figure 7C]. A flexible electronic skin with the dielectric Tetrapod-like ZnO whisker (T-ZnOw)/PDMS thin film sandwiched between two stretchable 3D hollow MXene spheres/Ag nanowires (AgNWs) hybrid nanocomposite electrodes could measure and distinguish contact parameters in real time [Figure 7D][73]. Stretchable electrodes are used as strain resistance modules to detect strain, while dielectric layers are used as pressure capacitance sensing modules to detect pressure.

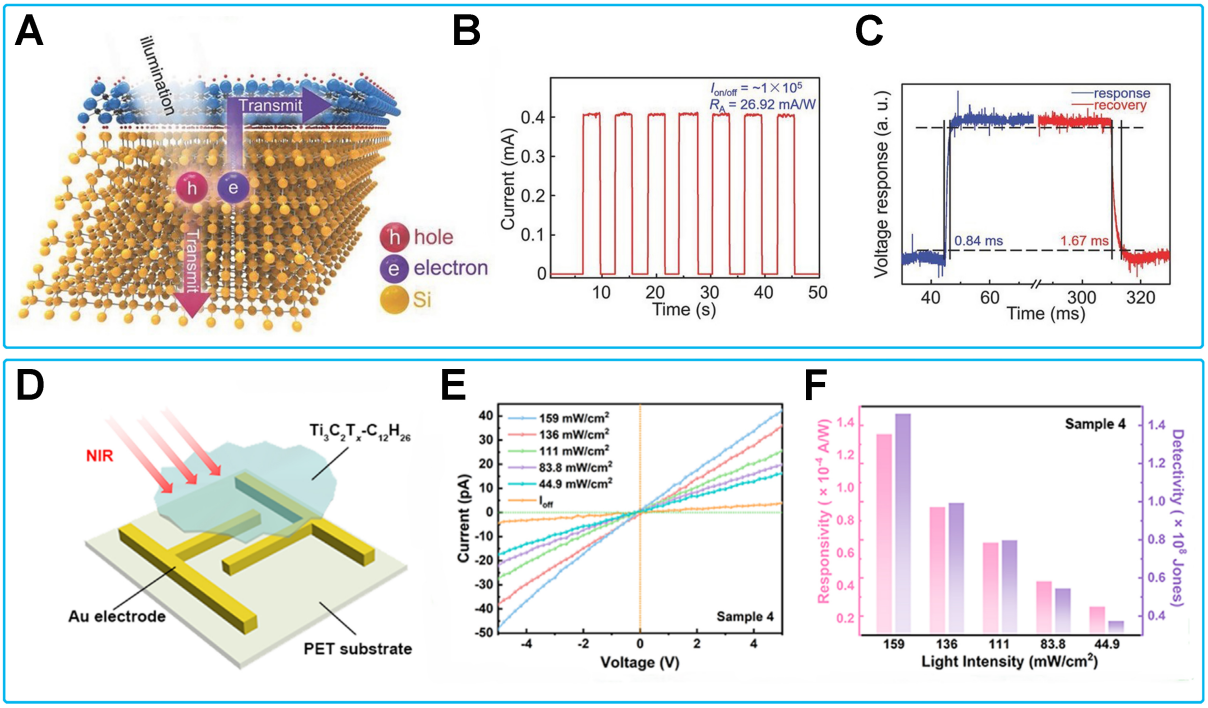

Figure 6. MXene-based photodetectors. (A) MXene-Si heterostructure; (B and C) Photoresponse performance of photodetectors with heterojunctions. Reproduced with permission[65]. Copyright 2017, Wiley; (D) $Ti_3C_2T_x$-$C_{12}H_{26}$-based photodetector; (E) I-V curves of photodetectors for 1064 nm lasers with different optical power densities; (F) Responsivity and detectivity of photodetectors. Reproduced with permission[67]. Copyright 2023, AIP Publishing. PET:Polyethylene terephthalate; $C_{12}H_{26}$: dodecyl.

Self-powered sensing systems offer viable solutions to address power supply issues[74]. In a self-powered pressure-strain sensor based on MXene triboelectric nanogenerator (TENG) [Figure 7E][75], strain of up to 400% can be detected from the increased resistance due to the gradual separation of initially wrinkled films. Meanwhile, pressure sensing is based on the piezoelectric effect of the film, which detects the intensified finger pressure from the increased contact area between the micro-wrinkled film and the finger.

Pressure/strain-temperature sensors

Different from stress/strain stimulation, temperature does not change the conductive network, but directly affects the movement of charge carriers within the material to change the resistance due to high Seebeck coefficient and good thermoelectric properties of MXenes[50,76]. As increased temperature produces more holes to accelerate the movement of charge carriers and decrease the resistance, MXene-based sensors often exhibit a negative temperature coefficient of resistance (TCR)[77].

Printing the MXene film on a polyethylene terephthalate substrate followed by encapsulation with a PDMS film fabricates a pressure-temperature dual-mode sensor without crosstalk [Figure 8A][78]. The temperature sensing layer is a non-porous MXene film with a hollow encapsulation layer that puts the sensing layer in direct contact with the external environment. The pressure sensing layer is a rectangular MXene film with square holes, and the encapsulating layer has a silver film at the corresponding hole locations. The negative TCR of MXene is compensated by the positive TCR of PDMS to provide the temperature-independent pressure sensing, whereas the PDMS encapsulation on top of the MXene temperature sensing layer prevents external pressure from directly acting on the MXene layer to eliminate the pressure effect. The stretchable dual-mode sensor that combines the electrically conductive MXene-AgNW and thermoelectric PEDOT:PSS-tellurium nanowire (TeNW) components could detect temperature (from 25 to 40 °C) from

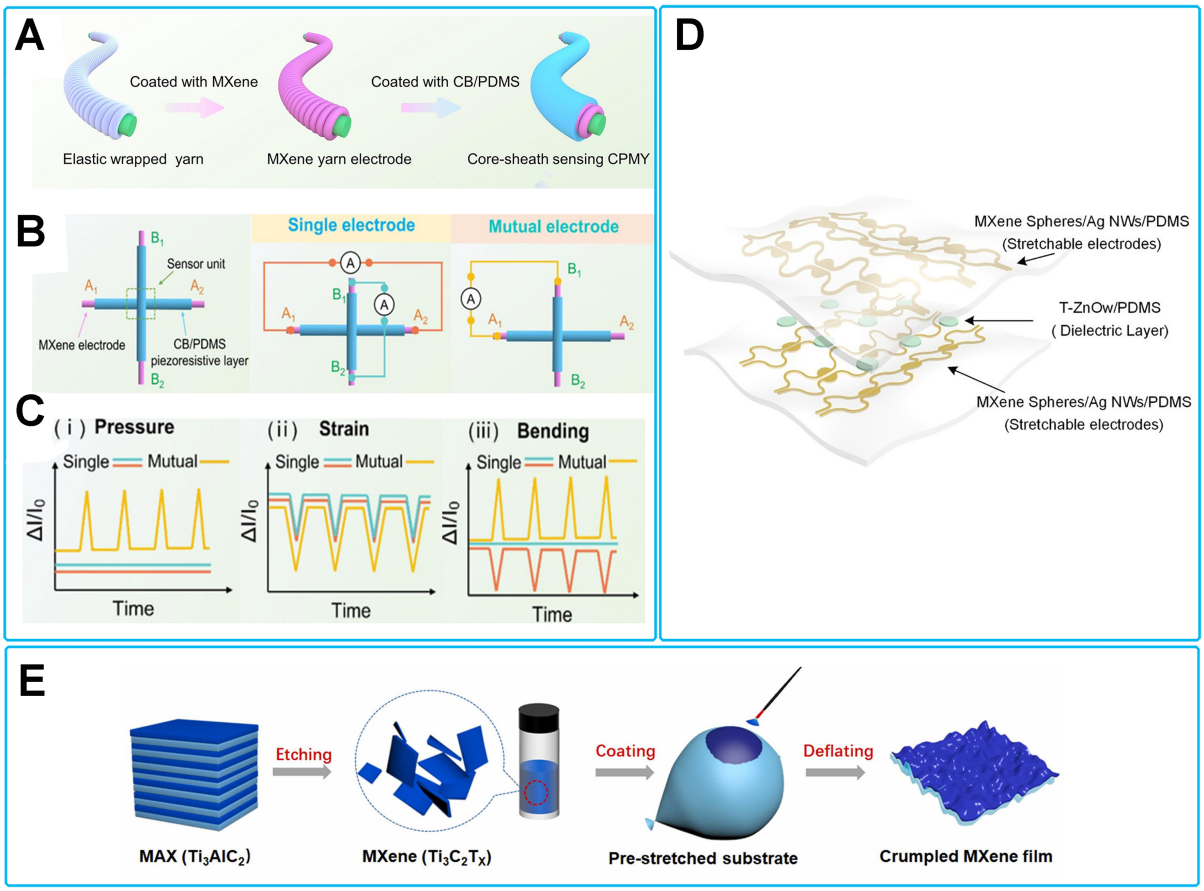

Figure 7. Pressure-Strain dual-mode sensors. (A) Fabrication of Pressure-Strain sensor; (B) Schematic of a typical sensor. Single electrode current and mutual electrode (sensor) current; (C) Current waveforms of different stimuli. Reproduced with permission[72]. Copyright 2024, Elsevier; (D) Structure diagram of electronic skin. Reproduced with permission[73]. Copyright 2021, American Chemical Society; (E) Schematic of crumpled MXene film fabrication process. Reproduced with permission[75]. Copyright 2021, Elsevier. PDMS: Polydimethylsiloxane; CB: carbon black; CPMY: carbon black/polydimethylsiloxane/MXene yarn; T-ZnOw: tetrapod-like ZnO whisker; AgNWs: Ag nanowires.

thermoelectric voltage and strain from the resistance without crosstalk[79]. By integrating Seebeck and piezoresistive effects, an elastic porous substrate modified with MXene provides a dual-modal sensor with decoupled sensing of temperature and pressure [Figure 8B][80]. Similarly, the resistance signal to measure pressure is not affected by temperature [Figure 8C], whereas the thermoelectric voltage generated by temperature is not affected by pressure because of the pressure-independent energy band of MXene [Figure 8D and E].

Pressure/strain-humidity sensors

With MXene integrated on a porous sponge skeleton, the dual-function flexible sensor can detect the absorbed water molecules (or humidity) from the increased resistance and the applied pressure from the decreased resistance[81]. The rubber-based flexible multifunctional sensor based on sodium polyacrylate (PAANa) between MXenes layers swells upon moisture and increases the resistance upon stretching due to cracks (sensitivity of 906.7 within the 98% strain range)[82]. The flexible sensor based on a composite material comprising MXenes, AgNWs, and tissue-like substrate can further enhanced humidity sensing due to promoted binding between water molecules and active sites on AgNWs (for reducing the activation energy)[83]. The sensor can also detect pressure from the decreased resistance due to increased conductivity

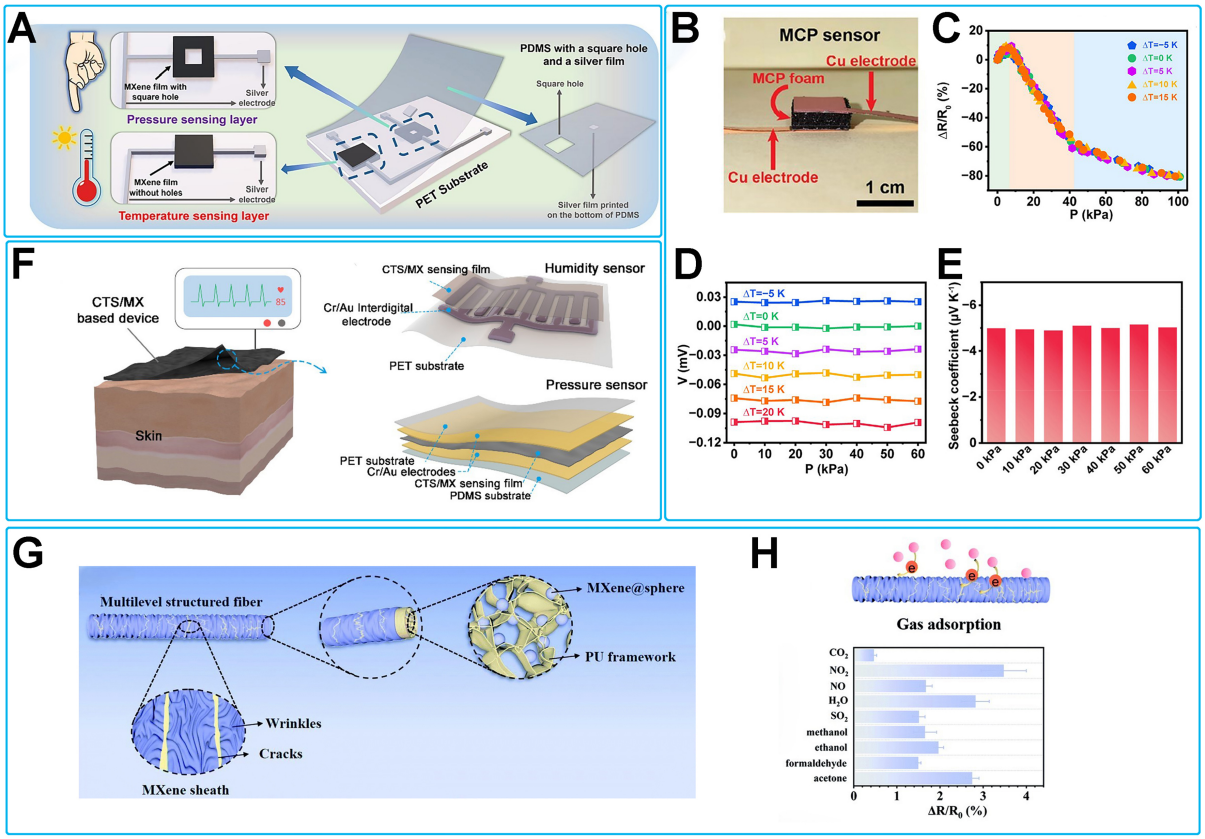

Figure 8. Dual-mode sensors. (A-E) Pressure-temperature sensor; (F) Pressure-humidity sensor; (G and H) Strain-gas sensor. (A) Pressure-temperature dual-mode sensor. Reproduced with permission[78]. Copyright 2024, Elsevier; (B) Schematic diagram of the sensor; (C) Temperature-independent pressure sensing; (D and E) Pressure-independent temperature sensing. Reproduced with permission[80]. Copyright 2023, American Chemical Society; (F) Schematic diagram of the structure of humidity and pressure sensors. Reproduced with permission[84]. Copyright 2021, American Chemical Society; (G) Schematic of multi-level structural fibers; (H) Response intensity of sensors to different gases. Reproduced with permission[89]. Copyright 2022, Royal Society of Chemistry. PET: Polyethylene terephthalate; PDMS: polydimethylsiloxane; MCP: MXene-decorated chitosan/PDMS; CTS: chitosan; MX: MXene; PU: polyurethane.

from pressure-induced decreases in the distance between the sensing layer and the electrode. Similarly, the MXene/chitosan film-based device exhibits responses to both pressure and humidity in the range from 11% to 95% RH even after 20 days [Figure 8F][84].

Pressure/strain-gas sensors

Besides distinguishing gas types/species, the detection of flow intensity or airflow[85,86] can help identify symptoms such as shortness of breath, difficulty in breathing, and irregular breathing caused by diseases such as influenza and pneumonia. By integrating $Ti_3C_2T_x$ nanoparticles onto the surface of PANI/bacterial cellulose (BC) nanofibers to increase gas adsorption and diffusion, the aerogel sensor exhibits increased NH_3 gas sensing due to enhanced efficacy in the protonation and deprotonation cycles of PANI[87]. The aerogel is also sensitive to pressure, with the decreased resistance to measure the increased pressure. In another porous flexible dual-modal sensor based on conductive composite of mesoporous silica-modified MXene and vanillin-modified polyacrylate and chitosan, the adsorbed NH_3 gas molecule with hydrogen bonds formed with the -OH and -F groups in MXene results in expansion of the polymeric substrate for reduced conductivity[88]. The mesoporous silica particles on the MXene surface also provide ample anchoring sites for ammonia molecules. Meanwhile, the deformation stacks up MXene to result in increased

resistance. A multi-level porous sensing fiber based on MXene and polyurethane (PU) expands after adsorbing gas and stretches the MXene sheath to increase the resistance [Figure 8G], with the response to different gases shown in Figure 8H[89]. This multi-level sensor achieves high strain sensitivity (from 174~298,000) and a wide strain sensing range (0%-150%).

MULTIMODAL FLEXIBLE SENSORS

Besides single- and dual-mode flexible sensors, multimode sensors have also been developed to recognize multiple complex stimuli in human motion and health for precise disease diagnosis. By innovatively introducing response functions to three or more stimuli, the resulting multimode sensors find enhanced detection ability and extended application scenarios. The performance parameters of MXene-based multimodal sensors are summarized and compared with other multimodal sensors based on different materials [Table 1].

Pressure-strain-temperature flexible sensors

With high biocompatibility and similar mechanical properties with biological tissues, conductive hydrogels reinforced with sodium carboxymethyl cellulose and MXene as multimodal sensors can detect strain (GF of 40.36 in 900%-1,000%), pressure (compressive strength of 2.2 MPa), and temperature (sensitivity of 2.5755 $°C^{-1}$ from 35 to 60 °C), along with supercapacitors (stability of 15,000 charge/discharge cycles)[98]. Introducing MXene-GO nanocomposites into organohydrogel also allows for direct sensing of strain (GF of 2.77), pressure(response time 712 ms, detection limit 100 mg), and temperature (TCR of 4.27 and 0.85 %/°C in 10-20 and 20-90 °C)[99]. Through pre-stretching and releasing, PPy nanowires (PpyNWs) as a nano-bridging layer are orthogonally arranged with MXene in a layer-by-layer manner and further tightly bonded on a vinyl hybridized silica nanoparticle-modified polyacrylamide (VSNP-PAM) hydrogel substrate provides the electronic skin with temperature (20-80 °C) and biaxial strain sensing (0%-2,800%) [Figure 9A and B][100]. The dielectric hydrogel sandwiched between PpyNWs and MXene also allows for tactile sensing from the pressure. Depositing 1D AgNWs and 2D MXene nanosheets onto fabrics modified by polydopamine (PDA, for enhance interactions with MXene) prepares multifunctional fabrics to detect strain (up to 445%), pressure (linearly from 2.5 to 10 kPa), and temperature (TCR of -0.08 %/°C in 25-126 °C) [Figure 9C][101].

Pressure/strain-temperature-humidity flexible sensors

To address the issues of unstable dispersibility and poor mechanical properties of MXenes, holocellulose nanofibrils-assisted intercalation has been exploited to obtain high-yield MXene inks via multiple freeze-thaw cycles[102], which can be printed on a variety of substrates to detect pressure/strain, temperature, humidity, and airflow. The flexible multifunctional electronic fabric sensing system can detect pressure (sensitivity of 1,529.1 kPa^{-1} over 150 kPa), temperature (0-65 °C), and humidity (sensitivity to humidity $R^2 > 0.99$) on the skin [Figure 9D][103]. Depositing thermochromic liquid crystals (with dye and color developer in solvent) on nonwoven fabric also enables visual temperature monitoring, as the dye and color developer separate with the increasing temperature to result in faded color [Figure 9E]. By integrating 2D MXene nanosheets and 1D AgNWs/cellulose nanofibers (CNF), the resulting electronic tattoo can precisely sense surface temperature changes, with the MXene/AgNWs network responding to 0.1% strain with a strain response time of 0.1 s, and facilitate humidity sensing and small changes in humidity (5%) can be detected due to hydrophilic functional moieties on CNF [Figure 9F][104].

Pressure/strain-electromagnetic-electrothermal sensor

Coating MXene and CNTs onto thermoplastic polyurethane (TPU) nonwoven fabrics, combined with a micro-crack structure formed by pre-stretching strategy, results in a strain sensor with extremely high sensitivity (GF of 9,022), a wide detection range (210%), fast response/recovery time (140/160 ms), and

Table 1. Performance comparison of multimodal sensors with different materials

Materials	Processing method	Performance	Advantages	Disadvantages	Ref.
CNT	1. Lithographic 2. Laser engraving 3. Spray coating 4. Dip coating 5. Spin coating 6. Blade coating 7. Layer-by-layer assembly	Pressure: S = 0.506 kPa^{-1} Temperature: TCR = -0.212% $°C^{-1}$ Humidity: S = 0.053%/%	1. Good electrical conductivity 2. High chemical and thermal stability 3. Various flexible macroscopic morphologies 4. Ease to be chemically functionalized	1. Inconclusive toxicity 2. Relatively high cost 3. Poor reproducibility among different devices 4. Poor stability	[90-92]
AgNWs	1. Electrospinning 2. Supersonic spraying 3. Vacuum filtration 4. Screen printed 5. Stencil-aided printing	Strain: GF = 155.3 Temperature: TCR = 0.2% $°C^{-1}$ Humidity: GF = 0.12	1. High stability 2. Flexibility 3. Bending resistance 4. Optical transparency 5. High conductivity	1. High cost 2. Large-area applications remain a challenge 3. Poor stability	[93,94]
LIG	1. Laser direct writing 2. Screen-printing 3. Hot-pressing	Pressure: S = 2.24 MPa^{-1} Temperature: S = -484.53 ppm $℃^{-1}$ Strain: S = 2.41	1. Fine tuning of laser parameters 2. Low costs and high chemical stability 3. Porous and cellular structures	1. Limited Resolution 2. Hard to further reduce the line width of LIG 3. Poor stretchability 4. Poor stability	[95,96]
MXene	1. Spray coating 2. Inkjet printing 3. Screen printing 4. Vacuum filtration 5. Layer-by-Layer composite 6. Surface coating	Pressure: ~100 MPa^{-1} Strain: GF = 5.23 Temperature: TCR = 0.44% $°C^{-1}$	1. Easy to process 2. Low cost 3. Hydrophilicity 4. Easy structure controllability 5. Large surface area	1. Poor dispersibility 2. Poor stability	[28,97]

CNT: Carbon nanotube; S: sensitivity; TCR: temperature coefficient of resistance; AgNWs: silver nanowires; GF: gauge factor; LIG: laser-induced graphene.

stability/durability (over 1,000 cycles) [Figure 9G][105]. Considering the use of MXene for EMI shielding and electrical Joule heating[106-109], the multifunctional electronic textiles also exhibit excellent EMI shielding effectiveness (~48 dB) and Joule heating (to 40/80/120 °C at 2/8/10 V) properties. With aqueous MXene/xanthan gum hybrid ink screen printed on paper substrate, the resulting multifunctional sensor exhibits excellent EMI shielding (shielding efficiency of up to 54.2 dB) and efficient Joule heating (heating rate of 20 °C/s and steady-state temperature of 130.8 °C at 4 V), along with pressure sensing (response time of < 130 ms and responds to pressures below30 kPa) [Figure 9H][110].

Optical-involved multimodal flexible sensors

MXenes have wide absorption band and energy levels and absorb photons across a broad wavelength range, which make it suitable for optical, photothermal (boosted by defect sites to promote electron-hole separation and transport), and photoelectrochemical applications[22,111]. By introducing Ca^{2+} and MXene nanosheets into a gellan gum/poly(N-hydroxyethyl acrylate) hydrogel matrix results in a conductive hydrogel with high photothermal conversion efficiency of 93.6% [Figure 10A][112]. With the concentration and temperature gradient of hot carriers generated in the photoexcited nanomaterials to drive the directional movement of carriers, the photoelectric response of open circuit voltage or short circuit current[113-115] allows the hydrogel to detect near-infrared light with good repeatability [Figure 10B]. Besides responding to pressure and strain, wearable device prepared by coating MXene, PDMS, and PDA on porous PU sponge membranes also exhibits photothermal conversion ability to increase the temperature from 25 to 80 °C within 40 s upon irradiation with near-infrared light for thermal therapy [Figure 10C][116]. Smart fibers and textiles prepared by 3D printing MXene-reinforced nanofibrillar cellulose also respond to photonic, electrical and mechanical stimuli [Figure 10D][117]. These textile strain sensors exhibited an excellent GF of 399.5 over a strain range of 8% to 10%. With 20 volts applied, the fibers reached a saturation temperature of

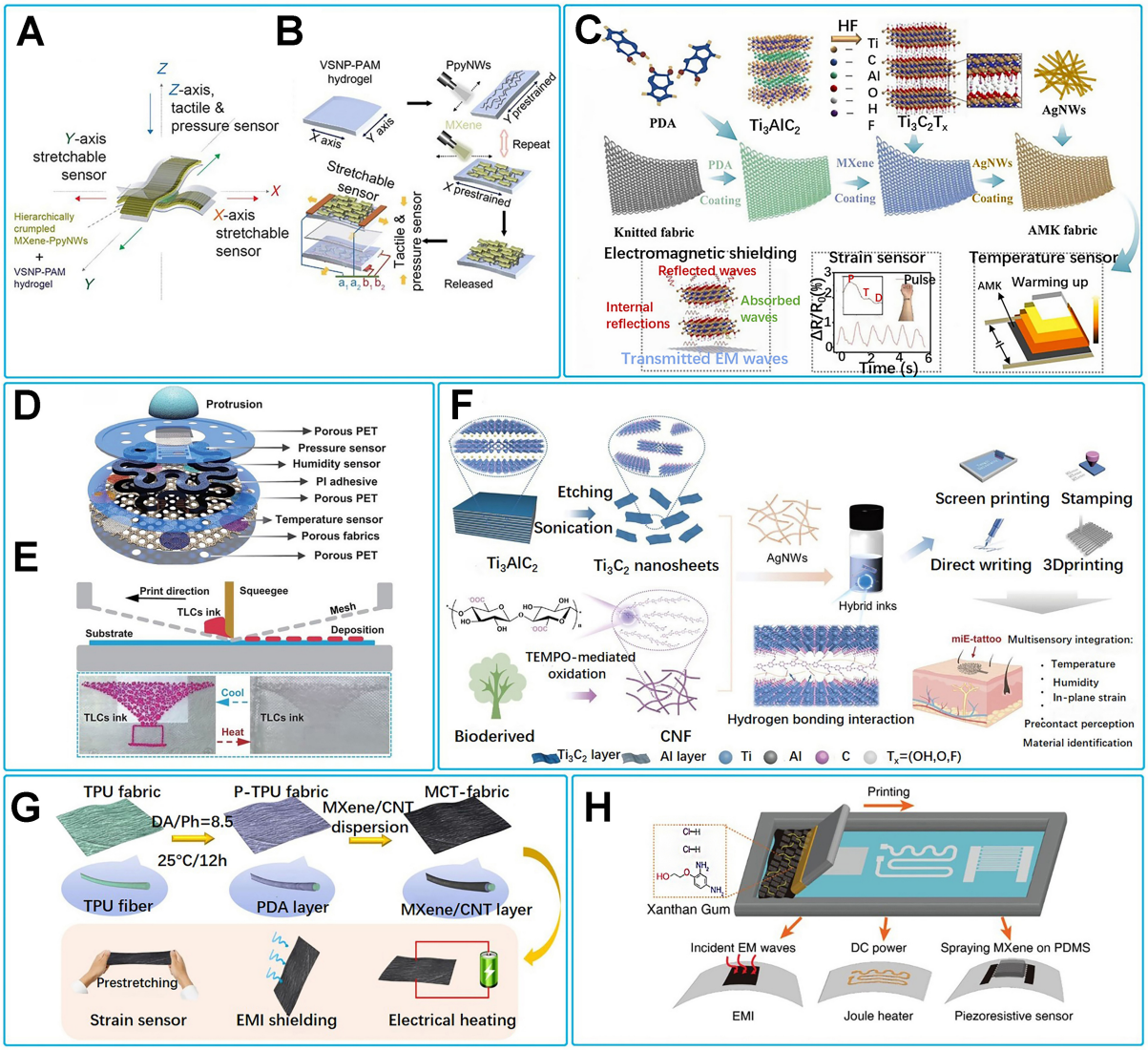

Figure 9. Multimodal flexible sensors. (A-C) Pressure-strain-temperature sensor; (D and E) Pressure-temperature-humidity sensor; (F) Strain-temperature-humidity sensor; (G and H) Pressure/strain-electromagnetic-electrothermal sensor. (A) Schematic diagram of the electronic skin; (B) Preparation of orthogonal arrangements of PpyNWs and MXene. Reproduced with permission[100]. Copyright 2020, Science; (C) Textiles fabrication. Reproduced with permission[101]. Copyright 2022, Elsevier; (D) The structure of the sensor; (E) Schematic of the temperature sensing mechanism. Reproduced with permission[103]. Copyright 2024, IPOSCIENCE; (F) Schematic of the electronic tattoo production. Reproduced with permission[104]. Copyright 2023, Wiley; (G) Multifunctional fabric manufacturing process. Reproduced with permission[105]. Copyright 2022, Elsevier; (H) Patterned screen-printed multifunction device[110]. Copyright 2022, Wiley. PpyNWs: Polypyrrole nanowires; VSNP-PAM: vinyl hybridized silica nanoparticle-modified polyacrylamide; PDA: polydopamine; AMK: AgNWs/MXene/PDA cross-linked PET knitted; AgNWs: Ag nanowires; TLCs: thermochromic liquid crystals; PET: polyethylene terephthalate; CNF: cellulose nanofibers; TPU: thermoplastic polyurethane; DA: dopamine hydrochloride; P-TPU: polydopamine-modified TPU; EMI: electromagnetic interference.

108.5 °C. And with 10 volts applied, the textile warmed to 72.3 °C in 300 s. In addition, under near-infrared light, the temperature of the fiber and textile could be increased to 62.2 and 80.6 °C, respectively.

APPLICATION OF MXENE-BASED SENSORS

Thanks to the unique high conductivity, ultra-thin flexibility and environmental response sensitivity of MXene materials, MXene-based flexible sensors are becoming a revolutionary technology in the field of

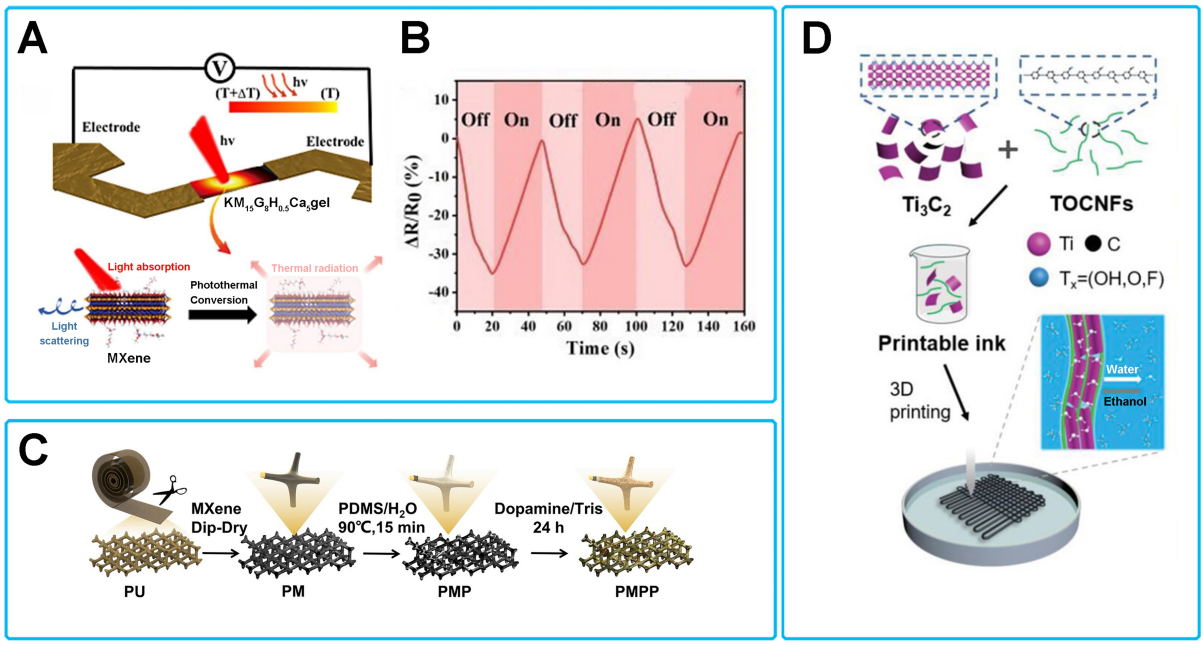

Figure 10. Optical-involved multimodal flexible sensors. (A) The principle of photothermoelectric effect conversion; (B) The response of the device to near-infrared light. Reproduced with permission[112]. Copyright 2024, Elsevier; (C) Nanocomposites manufacturing process. Reproduced with permission[116]. Copyright 2022, Nature; (D) Multifunctional fiber and textile manufacturing processes. Reproduced with permission[117]. Copyright 2019, Wiley. $KM_{15}G_8H_{0.5}Ca_5$ gel: The hydrogel formed by calcium chloride cross-linked gellan gum as the first network, poly(N-hydroxyethyl acrylate) as the second network, and 3-(trimethoxysilyl)propyl methacrylate -modified MXene nanosheets; TOCNFs: TEMPO (2,2,6,6-tetramethylpiperidine-1-oxylradi-cal)-mediated oxidized cellulose nanofibrils; PDMS: polydimethylsiloxane; PU: polyurethane; PM: MXene is assembled to the PU surface; PMP: PDMS are assembled to the PM surface; PMPP: the dopamine is covered over the PMP.

smart sensing. With the rapid development of the Internet of Things (IoT), smart healthcare and human-machine collaboration technologies, the market demand for high-performance flexible sensors continues to rise - these sensors not only need to adapt to complex deformations (e.g., folding, stretching, twisting), but also need to maintain stable operation in extreme environments. Currently, MXene-based sensors have deeply penetrated into the fields of medical and health monitoring, wearable electronics, environmental safety warning and human-computer interaction. In the medical field, it can monitor heart rate, breathing and other physiological signals in real time, helping chronic disease management and post-operative rehabilitation; in wearable devices, the thin and light sensor makes motion monitoring more comfortable; in environmental monitoring, it can accurately detect toxic gases in the air, guarding the environmental safety; and in the field of human-computer interaction, this sensor can also enhance the tactile sensitivity of robots and promote the development of intelligent prosthetic technology. The following section describes the innovative applications of MXene-based sensors in each of these four areas.

Healthcare

Pulse signals are important information for detecting cardiovascular disease. Flexible wearable sensors based on MXene are increasingly used for pulse detection. For example, MXene material was confined in the channels of fingerprint- microstructures and accordion-microstructures to prepare flexible piezoresistive pressure sensors with sensitivities as high as 99.5 kPa^{-1} and a detection limit of 9 Pa[118]. The sensors enable sensing of wrist impulses, sound, micromotion, and acceleration. Pulse measurement can be performed by attaching the sensor to the wrist of a volunteer. As shown in Figure 11A, the typical peaks of human pulse waveforms are clearly visible, i.e., the percussion wave (P-wave), the tidal wave (T-wave) and the diastolic wave (D-wave). The sensors have good application prospects in wearable medical monitoring devices, intelligent robots, and efficient human-machine interfaces.

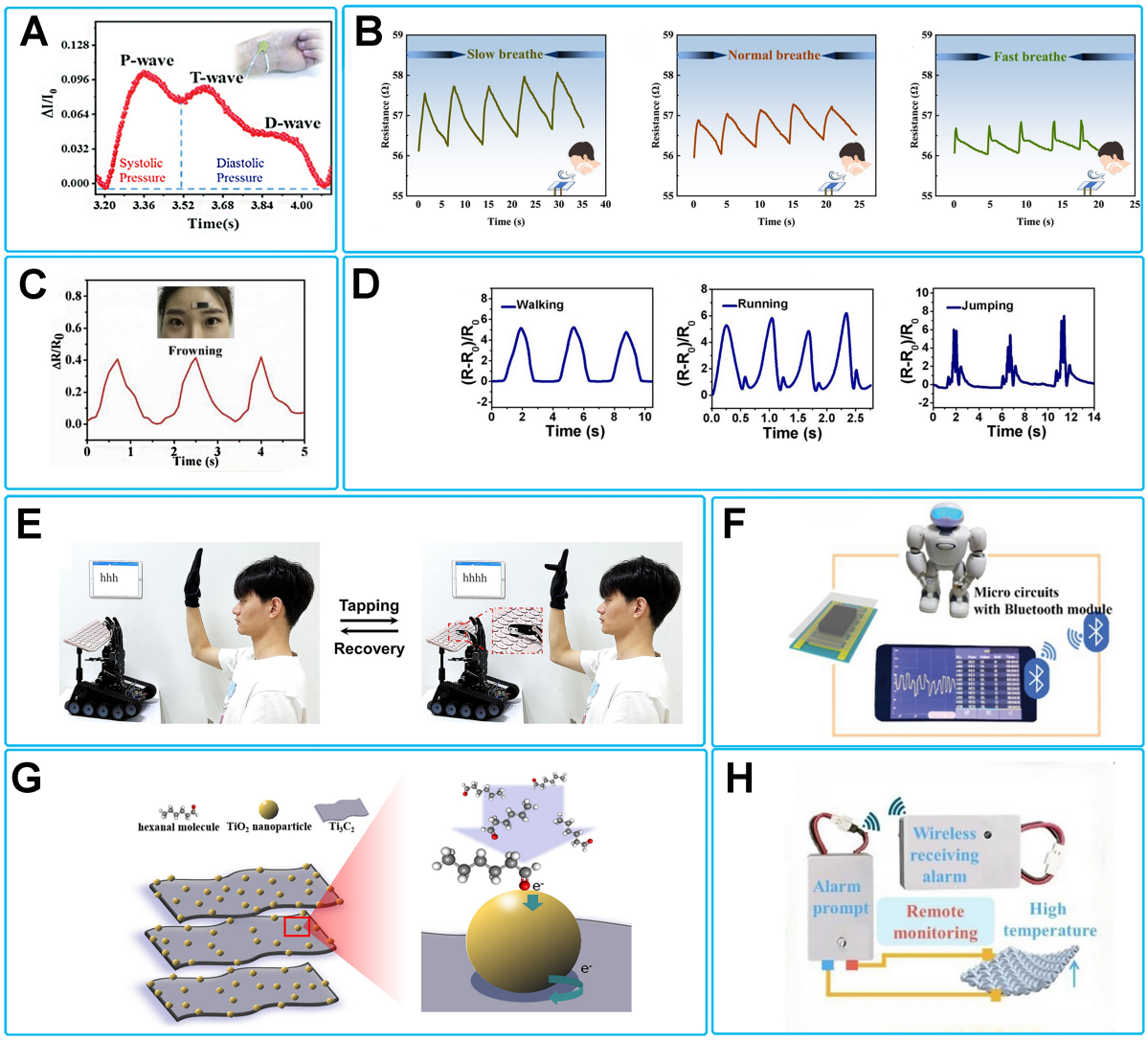

Figure 11. Various applications of MXene-based flexible sensors. (A) Measurement of pulse signals. Reproduced with permission[118]. Copyright 2020, Wiley; (B) Resistance signals for different respiration rates. Reproduced with permission[55]. Copyright 2024, Elsevier; (C) Wearable Sensor Detects Frowning Signals. Reproduced with permission[44]. Copyright 2020, Elsevier; (D) Sensors applied to large-scale motion detection. Reproduced with permission[45]. Copyright 2017. American Chemical Society; (E) Remotely manipulate a robotic hand to hit the keyboard. Reproduced with permission[119]. Copyright 2024, Elsevier; (F) Wireless monitoring of robot leg movements. Reproduced with permission[32]. Copyright 2019, Wiley; (G) Schematic diagram of the sensing mechanism of hexanal by composite materials. Reproduced with permission[120]. Copyright 2021, Elsevier; (H) Schematic diagram of a system with sensors embedded in fire suits for fire alarms. Reproduced with permission[121]. Copyright 2024, Springer Nature.

Respiratory rate is a key indicator for determining whether a person is healthy or not, and the breathing signal is generally monitored based on the impedance changes caused by the water molecules released during breathing, so the resistance fluctuations during breathing can be used to obtain the corresponding respiratory waveform. The inner layer is made of MXene material to achieve conductive function, while the outer layer employs CNF to enhance moisture absorption, a resistive humidity sensor imitating a hair rooted in the skin is designed, which achieves a humidity responsiveness of 117.93% in the range of 11% RH ~ 98% RH[55]. The sensor maintained stable sensing performance after exposure (7 days) or bending between

attempts. Figure 11B shows the characteristics of the respiratory waveform of human body at different respiration rates, by analyzing the resistive signals.

Wearable electronics

Flexible sensors can be used as wearable electronic devices to detect various signals from the human body. As society develops, there is an increasing need to monitor human activities. The MXene nanocomposite sensor based on tile-like stacked hierarchical microstructures achieved ultra-wide detection range (up to 80% strain) ultra-high sensitivity (GF = 2,369.1, strain > 40%) for sensing performance[44]. Figure 11C shows the strain sensor affixed to the forehead of a volunteer and the corresponding resistance increases when frowning. A wearable strain sensor based on $Ti_3C_2T_x$ MXene/carbon nanotube composites achieves an ultra-low detection limit of 0.1 % strain, high stretchability (up to 130 %), high sensitivity (regularization factor as high as 772.6), and tunable sensing range (30% ~ 130%)[45]. The extraordinary sensing performance enables the successful detection of substantial movements such as walking, running and jumping [Figure 11D].

Human-computer interaction

Traditional robots rely on rigid devices such as keyboards and joysticks for control, making the interaction process rigid and unintuitive. The introduction of flexible pressure sensors changes this traditional paradigm. By integrating flexible sensors into the touch interface (e.g., gloves or haptic panels), users can precisely control the robot hand with only natural gestures (e.g., light pressure, swiping). For example, a wearable electronic sensor was prepared by facile assembly combining MXene-enhanced biodegradable elastic sponges with MXene-printed interdigitated electrodes covered with breathable electrospun film. The sensor was mounted on the finger end of a robotic hand and remotely manipulated by a volunteer to monitor the tapping action of a Bluetooth keyboard. The sensor has promising applications in the fields of smart medical monitoring, human-computer interaction, smart personal protection and next-generation artificial skin [Figure 11E][119]. Flexible pressure sensors can be integrated into robots for sensing their interactions with people or other objects. For example, a composite sensor based on hollow MXene spheres/reduced graphene aerogel extends the sensitivity of the sensor (609 kPa^{-1} in the range of 6.4-10 kPa) through a 3D porous structure. As shown in Figure 11F, the sensor is attached to the robot leg, and the robot's leg motion can be monitored[32].

Environmental monitoring

Accelerated industrialization has made air pollution a serious threat to human health. Harmful gases such as carbon monoxide (CO), nitrogen oxides (NO_x) and volatile organic compounds (VOCs) not only damage the respiratory system, but may also cause serious illnesses such as cancer. Therefore, it is of great significance to prepare sensors that can monitor pollutants in the environment. Efficient detection of VOCs at room temperature was achieved by a facile hydrothermal synthesis of materials combining the high electrical conductivity of MXene with the catalytic activity of TiO_2[120]. $Ti_3C_2T_x$ - TiO_2 sensors exhibited enhanced responses of about 1.5-12.6 times over pure MXene sensors for the detection of a variety of VOCs at room temperature. As shown in Figure 11G, the sensor was responsive to hexanal, with the $Ti_3C_2T_x$ - TiO_2 sensor showing a gas response of approximately 3.4% for 10 ppm hexanal. The lower detection limit for hexanal gas is as low as 217 ppb.

In addition to the monitoring of gaseous pollutants, real-time temperature warning in extreme environments is also a key challenge for environmental safety, especially in high-risk scenarios such as fire rescue. While conventional temperature sensors often rely on external power sources and are difficult to wear out at high temperatures, MXene-based sensors based on self-repairing thermoelectric fibers offer an innovative solution for firefighting suit safety and protection. Preparation of "core-sheath" thermoelectric fibers using MXene as the thermoelectric core and self-healing silk sericin (SS)/oxide sodium alginate (OSA)

as a self-healing protective sheath. The device could trigger the high temperature warning within 1.17 s and achieved a self-healing rate of 89.12%. As shown in Figure 11H, It can be integrated into firefighting suits to achieve a wide range temperature sensing and repeatable high-temperature alarm performance at 200-400 °C without any external power supply[121].

CHALLENGES AND OPPORTUNITIES

Although MXenes show great potential for flexible sensing, there are still some serious challenges. For example: harsh synthesis conditions (e.g., fluoride etching), complex purification processes, and high precursor costs make the cost of scale-up production significantly higher than that of some cheaper materials. This economic bottleneck has limited the commercialization of MXenes. The oxidation resistance of MXene is not ideal, and prolonged exposure to the environment affects the performance of MXene-based devices. Therefore, addressing the oxygen resistance of MXene is critical for practical applications. Signal decoupling is one of the key technologies for implementing multi parameter detection in complex environments using MXene based flexible sensors. The current mainstream flexible sensors mainly focus on decoupling bimodal signals, and it is still difficult to achieve independent identification of three or more stimuli using a single sensing unit. If these challenges can be effectively addressed, MXene will change the future of flexible electronics.

While some of these challenges exist for MXene-based sensors, there are also some opportunities. It is worth noting that MXenes show advantages in some specific application scenarios due to their unique intrinsic properties and structural designability. For example, MXene-containing nanodevices exhibit superior EMI shielding and microwave attenuation performance at low loads and ultra-thin thicknesses, and MXene-based Joule heating devices exhibit excellent electrical and thermal conversion characteristics, as evidenced by excellent response times. In addition, theoretical calculations have shown that MXene exhibits significant potential advantages over other 2D materials in magnetism and optoelectronics applications. The MXene surface is rich in functional groups, which can be further optimized by chemical modification. This facilitates the integration of MXene into a wide range of sensors for improved device performance and multifunctional sensing. The excellent conductivity of MXene provides reliable electrical signal transmission guarantee for flexible electronic devices, especially when subjected to mechanical deformations such as bending and stretching, its layered structure can still maintain stable conductive paths. This characteristic is crucial for flexible electronic systems that require long-term stable operation, such as wearable devices and soft robots.

CONCLUSION AND OUTLOOK

With the advantages of unique layered 2D configuration, excellent electrical conductivity, high specific surface area, excellent hydrophilicity, and tunable morphology, they have been widely used in the fields of flexible sensors and wearable electronics. Significant progress has been made in flexible different-mode sensors prepared by coating MXene on substrate materials or compositing with other materials. This article reviews the latest research progress on MXene based sensors with different modes, introduces the applications of MXene based flexible sensors in different fields, and summarizes the challenges and opportunities currently faced by MXene and MXene based flexible sensors. In Table 2, some of the sensor structures and sensing mechanisms in the text are summarized.

In addition to addressing the above challenges and capitalizing on the opportunities, the future development of MXene-based flexible sensors will focus on the following trends:

Table 2. Summary of the structure and mechanism of the different modes of sensors

Sensor type	Structure	Mechanisms	Ref.
Single-modal	Sponge	Piezoresistive	[38]
	Porous	Piezoresistive	[39]
	Aerogel	Piezoresistive	[32]
	Sandwiched	Piezoresistive	[45]
	Polymer substrate	Thermoresistive	[51]
	"brick and mortar" structure	Resistive	[56]
Dual-modal	Yarn	Piezoresistive	[72]
	Crumpled	Piezoelectric	[75]
	Porous	Seebeck and piezoresistive	[80]
	Fiber	Resistive	[89]
Multimodal	Hydrogel	Piezoresistive - thermoresistive	[98]
	Fabric	Piezoresistive- thermoresistive	[101]
		Resistive-thermochromic liquid crystals	[103]
	Tatto	Resistive	[104]

Researchers should further understand the sensing and decoupling mechanisms of the sensors. Signal decoupling can be achieved by coupling multiple energy effects in the same sensor, adopting rational structural design, or with the help of machine learning algorithms. MXene composites with other materials such as carbon nanotubes, graphene, and conductive polymers, combined with surface functionalization or porous and layered structure design of MXene, form composite sensing materials with excellent performance and multifunctionality. This is an important direction for future research on sensing materials. Future multimodal sensors should be functionally integrated based on miniaturization and low cost. Meanwhile, flexibility and elasticity are crucial for wearable applications and electronic skin. Therefore, composite multifunctional sensitive materials to realize multifunctional sensing based on flexible materials such as hydrogels, aerogels, and elastic polymers have become a research hotspot in this field. With the selection of appropriate multifunctional materials and reasonable structural design to achieve multifunctional sensing, and the deep integration of IoT and artificial intelligence technologies, MXene-based flexible sensors are expected to achieve a higher level of integration, intelligence and multifunctionality.

DECLARATIONS

Authors' contributions

Wrote original draft: Yang, W.
Invistigation: Liu, F.; Lin, Y.; Yang, W.
Writing-review and editing: Wang, J.; Cheng, H.
Funding acquisition: Wang, J.; Chen, H.
Visualization: Zhang, C.
Supervision: Chen, H.

Availability of data and materials

The datasets generated or analyzed during this study are available from the corresponding authors upon reasonable request.

Financial support and sponsorship

This work was supported by the National Natural Science Foundation of China (Nos. 52201043, 12174172), the Natural Science Foundation of Fujian (Nos. 2024J011310, 2023J011396), Fuzhou Institute of Oceanography project (No. 2024F17), Fuzhou City Science and Technology Cooperation Project (2024-SG-008), and Fashu Charity Foundation of Minjiang University (MFK24024).

Conflicts of interest

Cheng, H. is a member of the Editorial Board of *Soft Science*. Cheng, H. was not involved in any steps of the editorial process, including reviewer selection, manuscript handling, or decision-making. The other authors declared that there are no conflicts of interest.

Ethical approval and consent to participate

Not applicable.

Consent for publication

Not applicable.

Copyright

REFERENCES

1. Zhao, Y.; Guo, X.; Hong, W.; et al. Biologically imitated capacitive flexible sensor with ultrahigh sensitivity and ultralow detection limit based on frog leg structure composites via 3D printing. *Compos. Sci. Technol.* **2023**, *231*, 109837. DOI
2. Hong, Q.; Liu, T.; Guo, X.; et al. 3D dual-mode tactile sensor with decoupled temperature and pressure sensing: toward biological skins for wearable devices and smart robotics. *Sens. Actuators. B. Chem.* **2024**, *404*, 135255. DOI
3. Zhu, P.; Wang, Y.; Wang, Y.; Mao, H.; Zhang, Q.; Deng, Y. Flexible 3D architectured piezo/thermoelectric bimodal tactile sensor array for E-skin application. *Adv. Energy. Mater.* **2020**, *10*, 2001945. DOI
4. Li, W. D.; Ke, K.; Jia, J.; et al. Recent advances in multiresponsive flexible sensors towards E-skin: a delicate design for versatile sensing. *Small* **2022**, *18*, e2103734. DOI PubMed
5. Haque, R. I.; Chandran, O.; Lani, S.; Briand, D. Self-powered triboelectric touch sensor made of 3D printed materials. *Nano. Energy.* **2018**, *52*, 54-62. DOI
6. Wei, X.; Liang, X.; Meng, C.; Cao, S.; Shi, Q.; Wu, J. Multimodal electronic textiles for intelligent human-machine interfaces. *Soft. Sci.* **2023**, *3*, 17. DOI
7. Zhang, X.; Tang, S.; Ma, R.; et al. High-performance multimodal smart textile for artificial sensation and health monitoring. *Nano. Energy.* **2022**, *103*, 107778. DOI
8. Chen, H.; Guo, S.; Zhang, S.; et al. Improved flexible triboelectric nanogenerator based on tile-nanostructure for wireless human health monitor. *Energy. Environ. Mater.* **2024**, *7*, e12654. DOI
9. Yang, C.; Zhang, D.; Wang, D.; Luan, H.; Chen, X.; Yan, W. In situ polymerized MXene/polypyrrole/hydroxyethyl cellulose-based flexible strain sensor enabled by machine learning for handwriting recognition. *ACS. Appl. Mater. Interfaces.* **2023**, *15*, 5811-21. DOI PubMed
10. Wang, Z.; Xu, Z.; Li, N.; Yao, T.; Ge, M. Flexible pressure sensors based on MXene/PDMS porous films. *Adv. Mater. Technol.* **2023**, *8*, 2200826. DOI
11. Liu, Z.; Tian, B.; Jiang, Z.; et al. Flexible temperature sensor with high sensitivity ranging from liquid nitrogen temperature to 1200 °C. *Int. J. Extrem. Manuf.* **2023**, *5*, 015601. DOI
12. Janica, I.; Montes-García, V.; Urban, F.; et al. Covalently functionalized MXenes for highly sensitive humidity sensors. *Small. Methods.* **2023**, *7*, e2201651. DOI PubMed
13. Lawaniya, S. D.; Kumar, S.; Yu, Y.; Rubahn, H.; Mishra, Y. K.; Awasthi, K. Functional nanomaterials in flexible gas sensors: recent progress and future prospects. *Mater. Today. Chem.* **2023**, *29*, 101428. DOI
14. Xu, T.; Song, Q.; Liu, K.; et al. Nanocellulose-assisted construction of multifunctional MXene-based aerogels with engineering biomimetic texture for pressure sensor and compressible electrode. *Nanomicro. Lett.* **2023**, *15*, 98. DOI PubMed PMC
15. Yang, C.; Wang, H.; Yang, J.; et al. A machine-learning-enhanced simultaneous and multimodal sensor based on moist-electric powered graphene oxide. *Adv. Mater.* **2022**, *34*, e2205249. DOI PubMed
16. Gu, J.; Huang, J.; Chen, G.; et al. Multifunctional poly(vinyl alcohol) nanocomposite organohydrogel for flexible strain and temperature sensor. *ACS. Appl. Mater. Interfaces.* **2020**, *12*, 40815-27. DOI PubMed
17. Qu, M.; Nilsson, F.; Qin, Y.; et al. Electrical conductivity and mechanical properties of melt-spun ternary composites comprising PMMA, carbon fibers and carbon black. *Compos. Sci. Technol.* **2017**, *150*, 24-31. DOI
18. Chang, K.; Li, L.; Zhang, C.; et al. Compressible and robust PANI sponge anchored with erected MXene flakes for human motion detection. *Compos. Part. A. Appl. Sci. Manuf.* **2021**, *151*, 106671. DOI
19. Wang, P.; Yu, W.; Li, G.; Meng, C.; Guo, S. Printable, flexible, breathable and sweatproof bifunctional sensors based on an all-nanofiber platform for fully decoupled pressure-temperature sensing application. *Chem. Eng. J.* **2023**, *452*, 139174. DOI
20. Han, M.; Shen, W.; Tong, X.; Corriou, J. Cellulose nanofiber/MXene/AgNWs composite nanopaper with mechanical robustness for high-performance humidity sensor and smart actuator. *Sens. Actuators. B. Chem.* **2024**, *406*, 135375. DOI
21. Lee, J.; Shin, S.; Lee, S.; et al. Highly sensitive multifilament fiber strain sensors with ultrabroad sensing range for textile electronics. *ACS. Nano.* **2018**, *12*, 4259-68. DOI PubMed

22. Hasan, M. M.; Hossain, M. M.; Chowdhury, H. K. Two-dimensional MXene-based flexible nanostructures for functional nanodevices: a review. *J. Mater. Chem. A.* **2021**, *9*, 3231-69. DOI
23. Peng, S.; Jin, Z.; Yao, Y.; et al. Metal-contact-induced transition of electrical transport in monolayer MoS_2: from thermally activated to variable-range hopping. *Adv. Elect. Materials.* **2019**, *5*, 1900042. DOI
24. Peng, S.; Zhang, J.; Jin, Z.; Zhang, D.; Shi, J.; Wei, S. Electric-field induced doping polarity conversion in top-gated transistor based on chemical vapor deposition of graphene. *Crystals* **2022**, *12*, 184. DOI
25. Zhang, L.; Zhang, S.; Wang, C.; Zhou, Q.; Zhang, H.; Pan, G. B. Highly sensitive capacitive flexible pressure sensor based on a high-permittivity MXene nanocomposite and 3D network electrode for wearable electronics. *ACS. Sens.* **2021**, *6*, 2630-41. DOI PubMed
26. Wang, T.; Qiu, Z.; Li, H.; et al. High sensitivity, wide linear-range strain sensor based on MXene/AgNW composite film with hierarchical microcrack. *Small* **2023**, *19*, e2304033. DOI PubMed
27. Gogotsi, Y.; Anasori, B. The rise of MXenes. *ACS. Nano.* **2019**, *13*, 8491-4. DOI PubMed
28. Du, T.; Han, X.; Yan, X.; et al. MXene-based flexible sensors: materials, preparation, and applications. *Adv. Mater. Technol.* **2023**, *8*, 2202029. DOI
29. Qiao, H.; Qin, W.; Chen, J.; et al. AuCu decorated MXene/RGO aerogels towards wearable thermal management and pressure sensing applications. *Mater. Des.* **2023**, *228*, 111814. DOI
30. Cao, W.; Ouyang, H.; Xin, W.; et al. A stretchable highoutput triboelectric nanogenerator improved by MXene liquid electrode with high electronegativity. *Adv. Funct. Mater.* **2020**, *30*, 2004181. DOI
31. Xing, H.; Li, X.; Lu, Y.; et al. MXene/MWCNT electronic fabric with enhanced mechanical robustness on humidity sensing for real-time respiration monitoring. *Sens. Actuators. B. Chem.* **2022**, *361*, 131704. DOI
32. Zhu, M.; Yue, Y.; Cheng, Y.; et al. Hollow MXene sphere/reduced graphene aerogel composites for piezoresistive sensor with ultra□high sensitivity. *Adv. Elect. Materials.* **2020**, *6*, 1901064. DOI
33. Zhang, Z.; Weng, L.; Guo, K.; Guan, L.; Wang, X.; Wu, Z. Durable and highly sensitive flexible sensors for wearable electronic devices with PDMS-MXene/TPU composite films. *Ceram. Int.* **2022**, *48*, 4977-85. DOI
34. Ma, C.; Cao, W.; Zhang, W.; et al. Wearable, ultrathin and transparent bacterial celluloses/MXene film with Janus structure and excellent mechanical property for electromagnetic interference shielding. *Chem. Eng. J.* **2021**, *403*, 126438. DOI
35. Ma, C.; Ma, M.; Si, C.; Ji, X.; Wan, P. Flexible MXene-based composites for wearable devices. *Adv. Funct. Materials.* **2021**, *31*, 2009524. DOI
36. Tang, X.; Zhou, D.; Li, P.; et al. MXene-based dendrite-free potassium metal batteries. *Adv. Mater.* **2020**, *32*, e1906739. DOI PubMed
37. Abdolhosseinzadeh, S.; Schneider, R.; Verma, A.; Heier, J.; Nüesch, F.; Zhang, C. J. Turning Trash into treasure: additive free MXene sediment inks for screen-printed micro-supercapacitors. *Adv. Mater.* **2020**, *32*, e2000716. DOI PubMed
38. Xu, Z.; Zhang, D.; Li, Z.; et al. Waterproof flexible pressure sensors based on electrostatic self-assembled MXene/NH_2-CNTs for motion monitoring and electronic skin. *ACS. Appl. Mater. Interfaces.* **2023**, *15*, 32569-79. DOI PubMed
39. Ma, Y.; Yue, Y.; Zhang, H.; et al. 3D synergistical MXene/reduced graphene oxide aerogel for a piezoresistive sensor. *ACS. Nano.* **2018**, *12*, 3209-16. DOI PubMed
40. Yin, T.; Cheng, Y.; Hou, Y.; et al. 3D porous structure in MXene/PANI foam for a high-performance flexible pressure sensor. *Small* **2022**, *18*, e2204806. DOI PubMed
41. Cheng, Y.; Xie, Y.; Liu, Z.; et al. Maximizing electron channels enabled by MXene aerogel for high-performance self-healable flexible electronic skin. *ACS. Nano.* **2023**, 1393-402. DOI PubMed
42. Pu, J.; Zhao, X.; Zha, X.; et al. A strain localization directed crack control strategy for designing MXene-based customizable sensitivity and sensing range strain sensors for full-range human motion monitoring. *Nano. Energy.* **2020**, *74*, 104814. DOI
43. Taromsari S, Shi HH, Saadatnia Z, Park CB, Naguib HE. Design and development of ultra-sensitive, dynamically stable, multi-modal GnP@MXene nanohybrid electrospun strain sensors. *Chem. Eng. J.* **2022**, *442*, 136138. DOI
44. Chao, M.; Wang, Y.; Ma, D.; et al. Wearable MXene nanocomposites-based strain sensor with tile-like stacked hierarchical microstructure for broad-range ultrasensitive sensing. *Nano. Energy.* **2020**, *78*, 105187. DOI
45. Cai, Y.; Shen, J.; Ge, G.; et al. Stretchable $Ti_3C_2T_x$ MXene/carbon nanotube composite based strain sensor with ultrahigh sensitivity and tunable sensing range. *ACS. Nano.* **2018**, *12*, 56-62. DOI PubMed
46. Jeong, J.; Seok, H.; Shin, H.; Bin, C. S.; Kim, J.; Kim, H. Highly durable and conductive Korea traditional paper (Hanji) embedded with Ti3C2Tx MXene for Hanji-based paper electronics. *Nano. Energy.* **2024**, *131*, 110325. DOI
47. Wu, J.; Fan, X.; Liu, X.; et al. Highly sensitive temperature-pressure bimodal aerogel with stimulus discriminability for human physiological monitoring. *Nano. Lett.* **2022**, *22*, 4459-67. DOI PubMed
48. Peng, J.; Ge, F.; Han, W.; et al. MXene-based thermoelectric fabric integrated with temperature and strain sensing for health monitoring. *J. Mater. Sci. Technol.* **2025**, *212*, 272-80. DOI
49. Liu, L.; Yang, J.; Zhang, H.; Ma, J.; Zheng, J.; Wang, C. Recent advances of flexible MXene physical sensor to wearable electronics. *Mater. Today. Commun.* **2023**, *35*, 106014. DOI
50. Cao, Z.; Yang, Y.; Zheng, Y.; et al. Highly flexible and sensitive temperature sensors based on $Ti_3C_2T_x$ (MXene) for electronic skin. *J. Mater. Chem. A.* **2019**, *7*, 25314-23. DOI
51. Zhao, L.; Fu, X.; Xu, H.; Zheng, Y.; Han, W.; Wang, L. Tissue-like sodium alginate-coated 2D MXene-based flexible temperature sensors for full-range temperature monitoring. *Adv. Mater. Technol.* **2022**, *7*, 2101740. DOI

52. Sun, B.; Xu, G.; Ji, X.; et al. A strain-resistant flexible thermistor sensor array based on CNT/MXene hybrid materials for lithium-ion battery and human temperature monitoring. *Sens. Actuators. A. Phys.* **2024**, *368*, 115059. DOI
53. Yang, M.; Huang, M.; Li, Y.; et al. Printing assembly of flexible devices with oxidation stable MXene for high performance humidity sensing applications. *Sens. Actuators. B. Chem.* **2022**, *364*, 131867. DOI
54. Li, Y.; Huang, X.; Chen, Q.; Yao, Y.; Pan, W. Nanochitin/MXene composite coated on quartz crystal microbalance for humidity sensing. *Nanomaterials* **2023**, *13*, 3135. DOI PubMed PMC
55. Gong, G.; Lin, C.; Chen, W.; et al. Flexible cellulose nanofibers/MXene bilayer membrane humidity sensor with a synergistic effect of force and hygroscopic expansion. *Ceram. Int.* **2024**, *50*, 24670-8. DOI
56. Han, M.; Shen, W. Nacre-inspired cellulose nanofiber/MXene flexible composite film with mechanical robustness for humidity sensing. *Carbohydr. Polym.* **2022**, *298*, 120109. DOI PubMed
57. Huang, M.; Lu, J.; Ji, J.; et al. Non-contact humidity monitoring: boosting the performance of all-printed humidity sensor using PDDA-modified Ti3C2Tx nanoribbons. *Chem. Eng. J.* **2024**, *485*, 149633. DOI
58. Zhang, H.; Xu, X.; Huang, M.; et al. Interlayer cross-linked MXene enables ultra-stable printed paper-based flexible sensor for real-time humidity monitoring. *Chem. Eng. J.* **2024**, *495*, 153343. DOI
59. Li, Q.; Xu, M.; Jiang, C.; et al. Highly sensitive graphene-based ammonia sensor enhanced by electrophoretic deposition of MXene. *Carbon* **2023**, *202*, 561-70. DOI
60. Wang, Y.; Wang, Y.; Jian, M.; Jiang, Q.; Li, X. MXene key composites: a new arena for gas sensors. *Nanomicro. Lett.* **2024**, *16*, 209. DOI PubMed PMC
61. Yang, Z.; Lv, S.; Zhang, Y.; et al. Self-assembly 3D porous crumpled MXene spheres as efficient gas and pressure sensing material for transient all-MXene sensors. *Nanomicro. Lett.* **2022**, *14*, 56. DOI PubMed PMC
62. Jin, L.; Wu, C.; Wei, K.; et al. Polymeric Ti_3C_2Tx MXene composites for room temperature ammonia sensing. *ACS. Appl. Nano. Mater.* **2020**, *3*, 12071-9. DOI
63. Wu, G.; Du, H.; Pakravan, K.; et al. Polyaniline/$Ti_3C_2T_x$ functionalized mask sensors for monitoring of CO_2 and human respiration rate. *Chem. Eng. J.* **2023**, *475*, 146228. DOI
64. Yang, Z.; Jiang, L.; Wang, J.; et al. Flexible resistive NO_2 gas sensor of three-dimensional crumpled MXene $Ti_3C_2T_x$/ZnO spheres for room temperature application. *Sens. Actuators. B. Chem.* **2021**, *326*, 128828. DOI
65. Kang, Z.; Ma, Y.; Tan, X.; et al. Mxene-silicon van der waals heterostructures for high-speed self-driven photodetectors. *Adv. Elect. Mater.* **2017**, *3*, 1700165. DOI
66. Chertopalov, S.; Mochalin, V. N. Environment-sensitive photoresponse of spontaneously partially oxidized Ti_3C_2 MXene thin films. *ACS. Nano.* **2018**, *12*, 6109-16. DOI PubMed
67. Hu, C.; Du, Z.; Wei, Z.; Li, L.; Shen, G. Functionalized Ti_3C_2Tx MXene with layer-dependent band gap for flexible NIR photodetectors. *Appl. Phys. Rev.* **2023**, *10*, 021402. DOI
68. Chen, J.; Zhu, Y.; Chang, X.; et al. Recent progress in essential functions of soft electronic skin. *Adv. Funct. Mater.* **2021**, *31*, 2104686. DOI
69. Luo, H.; Pang, G.; Xu, K.; Ye, Z.; Yang, H.; Yang, G. A fully printed flexible sensor sheet for simultaneous proximity-pressure-temperature detection. *Adv. Mater. Technol.* **2021**, *6*, 2100616. DOI
70. Chen, Y.; Gao, Z.; Zhang, F.; Wen, Z.; Sun, X. Recent progress in self-powered multifunctional e-skin for advanced applications. *Exploration* **2022**, *2*, 20210112. DOI PubMed PMC
71. Deng, S.; Li, Y.; Li, S.; et al. A multifunctional flexible sensor based on PI-MXene/$SrTiO_3$ hybrid aerogel for tactile perception. *Innovation* **2024**, *5*, 100596. DOI PubMed PMC
72. Yu, Q.; Pan, J.; Jiang, Z.; Guo, Z.; Jiang, J. Stretchable multimodal textile sensor based on core-sheath CB/PDMS/MXene sensing yarn for efficiently distinguishing mechanical stimulus. *Chem. Eng. J.* **2024**, *493*, 152462. DOI
73. Zhao, X. F.; Wen, X. H.; Zhong, S. L.; et al. Hollow MXene sphere-based flexible E-skin for multiplex tactile detection. *ACS. Appl. Mater. Interfaces.* **2021**, *13*, 45924-34. DOI PubMed
74. Ma, M.; Zhang, Z.; Zhao, Z.; et al. Self-powered flexible antibacterial tactile sensor based on triboelectric-piezoelectric-pyroelectric multi-effect coupling mechanism. *Nano. Energy.* **2019**, *66*, 104105. DOI
75. Cao, Y.; Guo, Y.; Chen, Z.; et al. Highly sensitive self-powered pressure and strain sensor based on crumpled MXene film for wireless human motion detection. *Nano. Energy.* **2022**, *92*, 106689. DOI
76. Wang, P.; Liu, G.; Sun, G.; Meng, C.; Shen, G.; Li, Y. An integrated bifunctional pressure-temperature sensing system fabricated on a breathable nanofiber and powered by rechargeable zinc-air battery for long-term comfortable health care monitoring. *Adv. Fiber. Mater.* **2024**, *6*, 1037-52. DOI
77. Zhao, T.; Liu, H.; Yuan, L.; et al. A multi-responsive MXene-based actuator with integrated sensing function. *Adv. Materials. Inter.* **2022**, *9*, 2101948. DOI
78. Yuan, T.; Yin, R.; Li, C.; Fan, Z.; Pan, L. $Ti_3C_2T_x$ MXene-based all-resistive dual-mode sensor with near-zero temperature coefficient of resistance for crosstalk-free pressure and temperature detections. *Chem. Eng. J.* **2024**, *487*, 150396. DOI
79. Li, F.; Liu, Y.; Shi, X.; et al. Printable and stretchable temperature-strain dual-sensing nanocomposite with high sensitivity and perfect stimulus discriminability. *Nano. Lett.* **2020**, *20*, 6176-84. DOI PubMed
80. Gao, F. L.; Liu, J.; Li, X. P.; et al. Ti_3C_2Tx MXene-based multifunctional tactile sensors for precisely detecting and distinguishing temperature and pressure stimuli. *ACS. Nano.* **2023**, *17*, 16036-47. DOI PubMed

81. Xu, Y.; Qiang, Q.; Zhao, Y.; et al. A super water-resistant MXene sponge flexible sensor for bifunctional sensing of physical and chemical stimuli. *Lab. Chip.* **2023**, *23*, 485-94. DOI PubMed
82. Yang, Y.; Kong, L.; Huang, B.; Lin, B.; Fu, L.; Xu, C. A high-sensitive rubber-based sensor with integrated strain and humidity responses enabled by bionic gradient structure. *Adv. Funct. Mater.* **2024**, *34*, 2400789. DOI
83. Xu, H.; Zheng, Y.; Yuan, Z.; Lou, Z.; Wang, L.; Han, W. High-performance flexible dual-function networks based on MXene hybrid film for human-machine interaction. *J. Phys. D:. Appl. Phys.* **2023**, *56*, 084004. DOI
84. Wang, L.; Wang, D.; Wang, K.; Jiang, K.; Shen, G. Biocompatible MXene/chitosan-based flexible bimodal devices for real-time pulse and respiratory rate monitoring. *ACS. Materials. Lett.* **2021**, *3*, 921-9. DOI
85. Kumar, A.; Kumar, R. R.; Shaikh, M. O.; et al. Wearable strain sensor utilizing the synergistic effect of $Ti_3C_2T_x$ MXene/AgNW nanohybrid for point-of-care respiratory monitoring. *Mater. Today. Chem.* **2024**, *37*, 102024. DOI
86. Wang, J.; Zhang, D.; Wang, D.; et al. Efficient fabrication of TPU/MXene/tungsten disulfide fibers with ultra-fast response for human respiratory pattern recognition and disease diagnosis via deep learning. *ACS. Appl. Mater. Interfaces.* **2023**, *15*, 37946-56. DOI PubMed
87. Zhi, H.; Zhang, X.; Wang, F.; Wan, P.; Feng, L. Flexible Ti_3C_2Tx MXene/PANI/bacterial cellulose aerogel for e-Skins and gas sensing. *ACS. Appl. Mater. Interfaces.* **2021**, *13*, 45987-94. DOI PubMed
88. Ni, Y.; Chen, J.; Chen, K. Flexible vanillin-polyacrylate/chitosan/mesoporous nanosilica-MXene composite film with self-healing ability towards dual-mode sensors. *Carbohydr. Polym.* **2024**, *335*, 122042. DOI PubMed
89. Guo, Q.; Pang, W.; Xie, X.; Xu, Y.; Yuan, W. Stretchable, conductive and porous MXene-based multilevel structured fibers for sensitive strain sensing and gas sensing. *J. Mater. Chem. A.* **2022**, *10*, 15634-46. DOI
90. Sharma, S.; Pradhan, G. B.; Jeong, S.; et al. Stretchable and all-directional strain-insensitive electronic glove for robotic skins and human-machine interfacing. *ACS. Nano.* **2023**, *17*, 8355-66. DOI PubMed
91. Palumbo, A.; Li, Z.; Yang, E. H. Trends on carbon nanotube-based flexible and wearable sensors via electrochemical and mechanical stimuli: a review. *IEEE. Sensors. J.* **2022**, *22*, 20102-25. DOI
92. Wang, R.; Sun, L.; Zhu, X.; et al. Carbon nanotube-based strain sensors: structures, fabrication, and applications. *Adv. Mater. Technol.* **2023**, *8*, 2200855. DOI
93. Wei, C.; Zhou, H.; Wang, Z.; et al. Transient flexible multimodal sensors based on degradable fibrous nanocomposite mats for monitoring strain, temperature, and humidity. *ACS. Appl. Polym. Mater.* **2024**, *6*, 4014-24. DOI
94. Sharma, N.; Nair, N. M.; Nagasarvari, G.; et al. A review of silver nanowire-based composites for flexible electronic applications. *Flex. Print. Electron.* **2022**, *7*, 014009. DOI
95. Qin, H.; Hajiaghajani, A.; Escobar, A. R.; et al. Laser-induced graphene-based smart textiles for wireless cross-body metrics. *ACS. Appl. Nano. Mater.* **2023**, *6*, 19158-67. DOI
96. Xu, K.; Cai, Z.; Luo, H.; et al. Toward integrated multifunctional laser-induced graphene-based skin-like flexible sensor systems. *ACS. Nano.* **2024**, *18*, 26435-76. DOI PubMed
97. He, P.; Guo, R.; Hu, K.; et al. Tough and super-stretchable conductive double network hydrogels with multiple sensations and moisture-electric generation. *Chem. Eng. J.* **2021**, *414*, 128726. DOI
98. Yin, H.; Liu, F.; Abdiryim, T.; Chen, J.; Liu, X. Sodium carboxymethyl cellulose and MXene reinforced multifunctional conductive hydrogels for multimodal sensors and flexible supercapacitors. *Carbohydr. Polym.* **2024**, *327*, 121677. DOI PubMed
99. Hu, K.; Zhao, Z.; Wang, Y.; et al. A tough organohydrogel-based multiresponsive sensor for a triboelectric nanogenerator and supercapacitor toward wearable intelligent devices. *J. Mater. Chem. A.* **2022**, *10*, 12092-103. DOI
100. Cai, Y.; Shen, J.; Yang, C. W.; et al. Mixed-dimensional MXene-hydrogel heterostructures for electronic skin sensors with ultrabroad working range. *Sci. Adv.* **2020**, *6*, eabb5367. DOI PubMed PMC
101. Zhao, W.; Zheng, Y.; Qian, J.; et al. AgNWs/MXene derived multifunctional knitted fabric capable of high electrothermal conversion efficiency, large strain and temperature sensing, and EMI shielding. *J. Alloys. Compd.* **2022**, *923*, 166471. DOI
102. Chen, Y.; Li, Y.; Liu, Y.; Chen, P.; Zhang, C.; Qi, H. Holocellulose nanofibril-assisted intercalation and stabilization of $Ti_3C_2T_x$ MXene inks for multifunctional sensing and EMI shielding applications. *ACS. Appl. Mater. Interfaces.* **2021**, *13*, 36221-31. DOI PubMed
103. Zhao, Y.; Yuan, Y.; Zhang, H.; et al. A fully integrated electronic fabric-enabled multimodal flexible sensors for real-time wireless pressure-humidity-temperature monitoring. *Int. J. Extrem. Manuf.* **2024**, *6*, 065502. DOI
104. Wang, Z.; Zhou, Z.; Li, C. L.; et al. A single electronic tattoo for multisensory integration. *Small. Methods.* **2023**, *7*, e2201566. DOI PubMed
105. Zhang, D.; Yin, R.; Zheng, Y.; et al. Multifunctional MXene/CNTs based flexible electronic textile with excellent strain sensing, electromagnetic interference shielding and Joule heating performances. *Chem. Eng. J.* **2022**, *438*, 135587. DOI
106. Yang, Y.; Li, B.; Wu, N.; et al. Biomimetic porous MXene-based hydrogel for high-performance and multifunctional electromagnetic interference shielding. *ACS. Materials. Lett.* **2022**, *4*, 2352-61. DOI
107. Wang, H.; Jiang, Y.; Ma, Z.; et al. Hyperelastic, robust, fire-safe multifunctional MXene aerogels with unprecedented electromagnetic interference shielding efficiency. *Adv. Funct. Mater.* **2023**, *33*, 2306884. DOI
108. Zhu, Y.; Liu, J.; Guo, T.; Wang, J. J.; Tang, X.; Nicolosi, V. Multifunctional Ti_3C_2Tx MXene composite hydrogels with strain sensitivity toward absorption-dominated electromagnetic-interference shielding. *ACS. Nano.* **2021**, *15*, 1465-74. DOI PubMed
109. Luo, J.; Gao, S.; Luo, H.; et al. Superhydrophobic and breathable smart MXene-based textile for multifunctional wearable sensing

electronics. *Chem. Eng. J.* **2021**, *406*, 126898. DOI

110. Wu, H.; Xie, Y.; Ma, Y.; et al. Aqueous MXene/xanthan gum hybrid inks for screen-printing electromagnetic shielding, joule heater, and piezoresistive sensor. *Small* **2022**, *18*, e2107087. DOI PubMed
111. Zhu, X.; Zhang, Y.; Liu, M.; Liu, Y. 2D titanium carbide MXenes as emerging optical biosensing platforms. *Biosens. Bioelectron.* **2021**, *171*, 112730. DOI PubMed
112. Hou, M.; Yu, M.; Liu, W.; et al. Mxene hybrid conductive hydrogels with mechanical flexibility, frost-resistance, photothermoelectric conversion characteristics and their multiple applications in sensing. *Chem. Eng. J.* **2024**, *483*, 149299. DOI
113. Jiang, W.; Zheng, T.; Wu, B.; et al. A versatile photodetector assisted by photovoltaic and bolometric effects. *Light. Sci. Appl.* **2020**, *9*, 160. DOI PubMed PMC
114. Yang, S.; Jiao, S.; Nie, Y.; et al. Facile synthesis of bismuth nanoparticles for efficient self-powered broadband photodetector application. *J. Mater. Sci. Technol.* **2022**, *126*, 161-8. DOI
115. Zhang, Y.; Gong, M.; Wan, P. MXene hydrogel for wearable electronics. *Matter* **2021**, *4*, 2655-8. DOI
116. Wang, X.; Tao, Y.; Pan, S.; et al. Biocompatible and breathable healthcare electronics with sensing performances and photothermal antibacterial effect for motion-detecting. *npj. Flex. Electron.* **2022**, *6*, 228. DOI
117. Cao, W.; Ma, C.; Mao, D.; Zhang, J.; Ma, M.; Chen, F. MXene-reinforced cellulose nanofibril inks for 3D-printed smart fibres and textiles. *Adv. Funct. Mater.* **2019**, *29*, 1905898. DOI
118. Gao, Y.; Yan, C.; Huang, H.; et al. Microchannel□confined MXene based flexible piezoresistive multifunctional micro□force sensor. *Adv. Funct. Mater.* **2020**, *30*, 1909603. DOI
119. Huang, C.; Xiao, M.; Li, Z.; Fu, Z.; Shi, R. Bioinspired breathable biodegradable bioelastomer-based flexible wearable electronics for high-sensitivity human-interactive sensing. *Chem. Eng. J.* **2024**, *486*, 150013. DOI
120. Kuang, D.; Wang, L.; Guo, X.; et al. Facile hydrothermal synthesis of $Ti_3C_2T_x$-TiO_2 nanocomposites for gaseous volatile organic compounds detection at room temperature. *J. Hazard. Mater.* **2021**, *416*, 126171. DOI PubMed
121. Jiang, Q.; Wan, Y.; Qin, Y.; et al. Durable and wearable self-powered temperature sensor based on self-healing thermoelectric fiber by coaxial wet spinning strategy for fire safety of firefighting clothing. *Adv. Fiber. Mater.* **2024**, *6*, 1387-401. DOI